Highly efficient therapeutic gene editing of human hematopoietic stem cells

Yuxuan Wu[1,2,3,4,13], Jing Zeng[1,2,3,13], Benjamin P. Roscoe[5], Pengpeng Liu[5], Qiuming Yao[1,2,3,6,7], Cicera R. Lazzarotto[8], Kendell Clement[6,7], Mitchel A. Cole[1,2,3], Kevin Luk[5], Cristina Baricordi[1,2,3,9], Anne H. Shen[1,2,3], Chunyan Ren[1,2,3], Erica B. Esrick[1,2,3], John P. Manis[1,2,3], David M. Dorfman[10,11], David A. Williams[1,2,3], Alessandra Biffi[1,2,3,9], Carlo Brugnara [1,2,3], Luca Biasco[1,2,3,9,12], Christian Brendel[1,2,3,9], Luca Pinello[6,7], Shengdar Q. Tsai[8], Scot A. Wolfe[5] and Daniel E. Bauer [1,2,3]*

Re-expression of the paralogous γ-globin genes (*HBG1/2*) could be a universal strategy to ameliorate the severe β-globin disorders sickle cell disease (SCD) and β-thalassemia by induction of fetal hemoglobin (HbF, $\alpha_2\gamma_2$)[1]. Previously, we and others have shown that core sequences at the *BCL11A* erythroid enhancer are required for repression of HbF in adult-stage erythroid cells but are dispensable in non-erythroid cells[2–6]. CRISPR–Cas9-mediated gene modification has demonstrated variable efficiency, specificity, and persistence in hematopoietic stem cells (HSCs). Here, we demonstrate that Cas9:sgRNA ribonucleoprotein (RNP)-mediated cleavage within a GATA1 binding site at the +58 *BCL11A* erythroid enhancer results in highly penetrant disruption of this motif, reduction of BCL11A expression, and induction of fetal γ-globin. We optimize conditions for selection-free on-target editing in patient-derived HSCs as a nearly complete reaction lacking detectable genotoxicity or deleterious impact on stem cell function. HSCs preferentially undergo non-homologous compared with microhomology-mediated end joining repair. Erythroid progeny of edited engrafting SCD HSCs express therapeutic levels of HbF and resist sickling, while those from patients with β-thalassemia show restored globin chain balance. Non-homologous end joining repair-based *BCL11A* enhancer editing approaching complete allelic disruption in HSCs is a practicable therapeutic strategy to produce durable HbF induction.

Electroporation of Cas9 and single guide RNA (sgRNA) RNP complexes enables delivery of a transient pulse of genome editing material to human cells[7,8]. Previously, we had employed lentiviral-pooled sgRNA screening to identify a set of sgRNAs targeting the core of the +58 erythroid enhancer of *BCL11A,* resulting in potent HbF derepression[3]. We used in vitro transcription to produce sgRNAs targeting the *BCL11A* enhancer and electroporated RNP complexes to healthy donor CD34+ hematopoietic stem and progenitor cells (HSPCs), which resulted in variable editing

(9.5–87.0% indels; Extended Data Fig. 1a,b). Consistent with prior observations, chemically modified synthetic sgRNAs (MS-sgRNAs) produced more efficient editing than in vitro transcribed sgRNAs following RNP electroporation of CD34+ HSPCs[9]. We observed a dose-dependent relationship between RNP concentration and indel frequency and similar editing efficiency at Cas9:sgRNA molar ratios ranging from 1:1 to 1:2.5 (Extended Data Fig. 1c–e).

Of eight MS-sgRNAs targeting the core of the +58 erythroid enhancer of *BCL11A* in CD34+ HSPCs, editing efficiency ranged from 66.1–90.7% indel frequency (Fig. 1a,b and Extended Data Fig. 2). Editing with sgRNA-1617, which cleaves directly within a GATA1 binding motif[10] at the core of the +58 enhancer, gave the highest levels of γ-globin and HbF induction in erythroid progeny (Fig. 1a,c and Extended Data Fig. 1f,h). Editing of the *BCL11A* enhancer resulted in reduction in *BCL11A* transcript expression by 54.6% (Extended Data Fig. 1j). We observed a strong correlation between reduction of *BCL11A* expression and induction of γ-globin and HbF (Fig. 1d and Extended Data Fig. 1j-l). Deep sequencing confirmed the high rate of indels, and showed that the most common mutations were +1 base pair (bp) insertions, as produced by imprecise non-homologous end joining repair (NHEJ), followed by −15 bp and −13 bp deletions, each products of microhomology-mediated end joining (MMEJ) repair (Fig. 1f and Extended Data Figs. 1g and 2). We conducted clonal analysis of the erythroid progeny of CD34+ HSPCs edited at the *BCL11A* enhancer by sgRNA-1617, assessing genotype, globin gene expression by quantitative PCR with reverse transcription (RT–qPCR), and HbF analysis by HPLC (Extended Data Figs. 1i and 3d,e and Supplementary Table 1). Colonies with biallelic enhancer modifications demonstrated elevated γ-globin messenger RNA levels (mean 50.8% of total β-like globin, range 35.3–75.1%, compared with 14.7% in unedited colonies) and elevated HbF protein levels (mean 37.6%, range 27.5–46.9%, compared with 9.1% in unedited colonies). Single base insertions at the sgRNA-1617 cleavage site were just as effective as longer deletions at increasing HbF levels.

[1]Division of Hematology/Oncology, Boston Children's Hospital , Boston, MA, USA. [2]Department of Pediatric Oncology, Dana-Farber Cancer Institute, Boston, MA, USA. [3]Department of Pediatrics, Harvard Stem Cell Institute, Broad Institute of Harvard and MIT, Harvard Medical School, Boston, MA, USA. [4]Shanghai Key Laboratory of Regulatory Biology, Institute of Biomedical Sciences and School of Life Sciences, East China Normal University, Shanghai, China. [5]Department of Molecular, Cell and Cancer Biology, Li Weibo Institute for Rare Diseases Research, University of Massachusetts Medical School, Worcester, MA, USA. [6]Molecular Pathology Unit, Center for Cancer Research, and Center for Computational and Integrative Biology, Massachusetts General Hospital, Boston, MA, USA. [7]Department of Pathology, Broad Institute of Harvard and MIT, Harvard Medical School, Boston, MA, USA. [8]Department of Hematology, St. Jude Children's Research Hospital, Memphis, TN, USA. [9]Gene Therapy Program, Dana-Farber/Boston Children's Cancer and Blood Disorders Center, Boston, MA, USA. [10]Department of Pathology, Brigham and Women's Hospital , Boston, MA, USA. [11]Department of Pathology, Harvard Medical School, Boston, MA, USA. [12]University College of London, Great Ormond Street Institute of Child Health, Faculty of Population Health Sciences, London, UK. [13]These authors contributed equally: Yuxuan Wu, Jing Zeng. *e-mail: daniel.bauer@childrens.harvard.edu
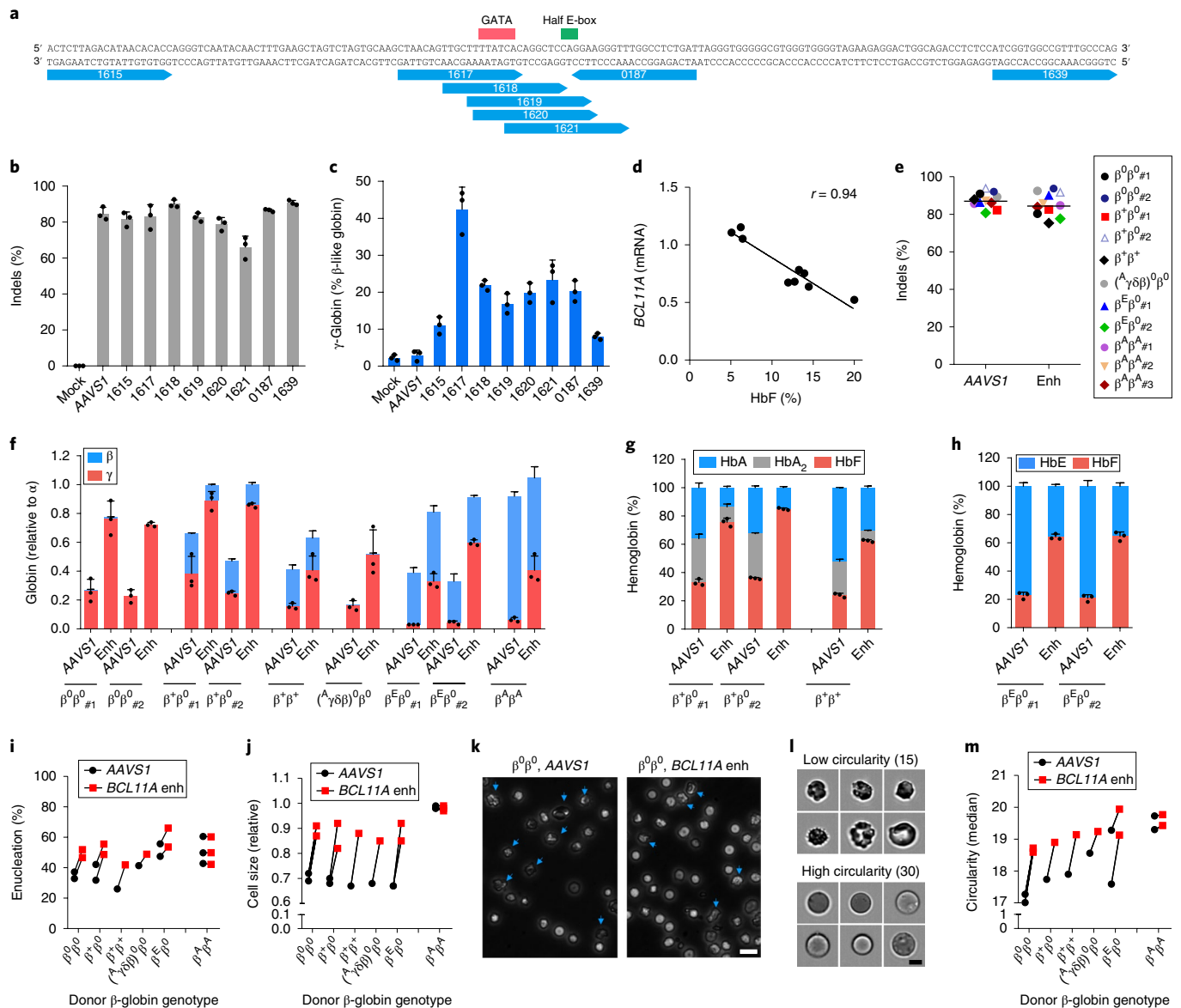
Fig. 1 | Identification of efficient *BCL11A* enhancer guide RNAs for HbF induction and amelioration of β-thalassemia. a, Eight MS-sgRNAs targeting *BCL11A* enhancer DNase I hypersensitive site (DHS) +58 functional core marked with blue arrows. GATA and Half E-box motifs marked with, respectively, red or green. **b**, Editing efficiency of Cas9 coupled with the various sgRNAs (each targeting *BCL11A* enhancer with exception of *AAVS1*) in CD34^{+} HSPCs measured by TIDE analysis. **c**, β-like globin expression by RT–qPCR analysis in erythroid cells in vitro differentiated from RNP edited CD34^{+} HSPCs. **d**, Correlation of *BCL11A* mRNA expression determined by RT–qPCR versus HbF by HPLC. Black dots represent samples edited with Cas9 coupled with different sgRNAs. The Pearson correlation coefficient (*r*) is shown. **e**, Editing efficiency as measured by TIDE analysis of Cas9:sgRNA RNP targeting *AAVS1* or *BCL11A* DHS +58 functional core (Enh) with MS-sgRNA-1617 in CD34^{+} HSPCs from patients with β-thalassemia or healthy donors (β[A]β[A]) of indicated β-globin genotypes. **f–h**, β-like globin expression by RT–qPCR normalized by α-globin (*P* = 0.00017 for *BCL11A* enhancer as compared with *AAVS1* edited for all comparisons as determined by unpaired two-tailed Student's *t*-tests), and HbF induction by HPLC analysis in erythroid cells that were in vitro differentiated. **i**, Enucleation of in vitro differentiated erythroid cells. **j**, Cell size measured by relative forward scatter intensity. **k**, Representative microscopy image showing rounder and more uniform appearance of enucleated erythroid cells following *BCL11A* enhancer editing. Blue arrows indicate poikilocytes. Scale bar, 15 μm. **l,m**, Imaging flow cytometry was used to establish a circularity index (**l**) and then to quantify (**m**) circularity of enucleated erythroid cells. Scale bar, 5 μm. In all graphs, data are plotted as mean ± s.d. and analyzed using unpaired two-tailed Student's *t*-tests. Data are representative of three biologically independent replicates.

To test if this *BCL11A* enhancer editing approach would result in clinically meaningful γ-globin induction, we edited CD34^{+} HSPCs from seven patients with β-thalassemia of varying genotypes, including β[0]β[0], β^{+}β[0], β^{+}β^{+}, (^Aγδβ)[0]β[0], and β[E]β[0] (Supplementary Table 2). The RNP editing rate with MS-sgRNA-1617 was similar to that from healthy control HSPCs (mean 84.4% indels; range 75.3–92.5%; Fig. 1e). RNP editing of the *AAVS1* locus served as a functionally neutral control. In each β-thalassemia donor's *BCL11A*

enhancer edited cells, we demonstrated potent induction of γ-globin (mean 63.6% relative to α-globin; range 33.0–89.0%; Fig. 1f) and induction of HbF fraction in donors with residual expression of HbA or HbE (Fig. 1g,h). We hypothesized that therapeutically relevant amelioration of globin chain imbalance, the pathophysiologic underpinning of β-thalassemia, would result in improvement of terminal erythroid maturation. We found a higher frequency of enucleation, larger size, and more circular shape of terminal erythroid cells

in each of the β-thalassemia samples, but no effect on the healthy donor samples, following *BCL11A* enhancer editing (Fig. 1i–m).

The durability of an autologous hematopoietic cell therapy depends on the ability to permanently modify stem cells. To test the impact of *BCL11A* enhancer editing on HSCs, we engrafted edited human CD34+ HSPCs into immunodeficient NBSGW mice, since they support not only myeloid and lymphoid, but also erythroid engraftment[11]. Using two separate donors, we found that the recipients of edited and unedited CD34+ HSPCs had similar levels of human lymphoid, myeloid, and erythroid cell engraftment within the bone marrow after 16 weeks (Extended Data Fig. 3a,c,d and Supplementary Table 3). We observed variability in the fraction of indels in the engrafting cells from edited mice, ranging from 13.8 to 85.5% (Extended Data Fig. 3b). Comparing the indel frequencies in the input cells with the engrafting cells we observed a mean reduction of 40.9%. In the engrafting bone marrow cells, we found no reduction in *BCL11A* transcript levels in edited B lymphocytes, but 80.0% reduction in edited erythroid cells, consistent with the strict lineage specificity of these enhancer sequences (Extended Data Fig. 3e,f). In human erythroid cells from the bone marrow, we observed robust induction of γ-globin, increasing from 1.8 to 46.8% after editing (Extended Data Fig. 3g). Edited bone marrow cells were able to support secondary transplantation to a similar level as unedited cells, while maintaining a mean indel frequency of 72.2%, consistent with gene editing of self-renewing HSCs (Extended Data Fig. 3h,i). Long-term engrafting HSCs not bearing biallelic therapeutic edits represent a possible barrier to full therapeutic benefit. In SCD a minority fraction of residual sickle erythrocytes can potentially result in negative rheologic and pathologic consequences[12,13]. Therefore we investigated methods to maximize editing efficiency in HSCs.

The SpCas9 protein we used in the experiments described above included two SV40 nuclear localization sequences (NLSs) on the carboxy (C) terminus[14] (subsequently called 2xNLS-Cas9). We hypothesized that additional orthogonal NLSs could improve genome editing efficiency. We appended a c-Myc-like NLS to the amino (N) terminus and both SV40 and nucleoplasmin NLSs to the C terminus of SpCas9 (subsequently called 3xNLS-Cas9) (Fig. 2a). We electroporated human CD34+ HSPCs with *BCL11A* enhancer-targeting RNPs at concentrations ranging from 1 to 10 μM and found increased indel frequencies at all doses with 3xNLS-Cas9 (Fig. 2b). At doses of 5 μM and greater the indel frequency exceeded 95%. The viability of cells electroporated with 3xNLS-Cas9 was inferior compared with those receiving 2xNLS-Cas9. However, as the concentration of 2xNLS-Cas9 was reduced, viability approached that of 3xNLS-Cas9-treated cells (Fig. 2c), suggesting that a component of the diluent for 2xNLS-Cas9 might be protective. The 2xNLS-Cas9 stock was dissolved in 10% glycerol, whereas the 3xNLS-Cas9 stock was not dissolved in glycerol. We electroporated cells with 3xNLS-Cas9 with a final glycerol concentration ranging from 0 to 8% and found that additional glycerol protected the cells from loss of viability (Fig. 2d). This protective effect was observed with 2xNLS-Cas9, 3xNLS-Cas9, and without Cas9, indicating that glycerol was protective against electroporation-mediated toxicity independent of genome editing (Fig. 2d). We observed similar protection against electroporation toxicity with glycine, consistent with a possible osmoprotectant effect (Extended Data Fig. 4a). There was a slight decrement of editing with increasing doses of glycerol, suggesting a balance between maximizing cell viability and genome editing efficiency (Fig. 2e). We found that 3xNLS-Cas9 RNP electroporation was able to achieve up to 98.1% indels in CD34+ HSPCs (Fig. 2f and Extended Data Fig. 4b,c). There was a similar distribution of alleles as with 2xNLS-Cas9 editing, with the +1 bp insertion the most frequent indel, followed by the −15 bp and −13 bp deletions. We observed a similar magnitude of decrease in *BCL11A* mRNA and protein level during in vitro erythroid maturation with 2xNLS-Cas9 or 3xNLS-Cas9 RNP electroporation, although there

was a modest increase in both γ-globin and HbF induction with 3xNLS-Cas9 (*P* < 0.05; Fig. 2g and Extended Data Fig. 4d–g).

We hypothesized that maximizing genome editing efficiency might increase the fraction of indels in engrafting edited HSCs and enhance HbF induction in erythroid progeny. RNP electroporation with 3xNLS-Cas9 and *BCL11A* enhancer MS-sgRNA-1617 resulted in similar human marrow engraftment after 16 weeks with edited and unedited CD34+ HSPCs, with a dose-dependent relationship between cell infusion dose and human cell engraftment (Fig. 2h and Extended Data Fig. 8b). We observed no difference in human engraftment if cells were infused 0, 1, or 2 d following electroporation (Extended Data Fig. 6a). Edited cells showed similar capacity for lymphoid, myeloid, and erythroid engraftment (Fig. 2i and Extended Data Fig. 5b,c). Engrafting human cells maintained 96.5% indels, similar to the 98.1% indels observed in the input cells (Fig. 2j and Extended Data Fig. 5d). In the bone marrow, *BCL11A* expression was preserved in edited B lymphocytes but reduced by 82.7% in edited erythroid cells (Fig. 2k,l). γ-Globin was elevated from 2.2% to 70.8% total β-like globin in edited human erythroid cells (Fig. 2m and Extended Data Fig. 5c). Transplant of CD34+ HSPCs electroporated with 3xNLS-Cas9 and MS-sgRNA-1617 and supplemented with 2%, 4% or 6% glycerol also yielded potent human engraftment while maintaining high indel frequencies in the repopulating cells (Extended Data Fig. 5e-h). The 3xNLS-Cas9 edited bone marrow cells were also able to support secondary transplantation to a similar level as unedited cells, while maintaining a mean indel frequency of 96.5%, consistent with gene editing of self-renewing HSCs (Fig. 2n,o and Extended Data Fig. 9d,e). The high efficiency of therapeutic editing within engrafting hematopoietic cells was consistently observed using HSPCs from four different healthy donors (Fig. 2h–o and Extended Data Fig. 5).

To test the specificity of the RNP sgRNA-1617, we performed CIRCLE-seq, a method to define genome-wide target sequences susceptible to RNP cleavage in vitro[15], identifying 20 potential off-target sites (Extended Data Fig. 6a and Supplementary Table 4). Amplicon deep sequencing of each of these 20 off-target sites from CD34+ HSPCs edited with both 2xNLS-Cas9 and 3xNLS-Cas9 did not identify any off-target sites at which we observed Cas9-dependent indels, at the limit of detection of 0.1% allele frequency (Extended Data Fig. 6b). From the same edited genomic DNA, we observed 81.0–95.5% on-target indels at the *BCL11A* enhancer. In addition, we tested, by amplicon deep sequencing, four additional in silico predicted off-target sites not identified by CIRCLE-seq (Supplementary Table 5) and did not detect indels (Extended Data Fig. 6b). Recent studies have emphasized that p53 is induced following programmable nuclease-mediated DNA cleavage[16,17]. Consistent with intact DNA damage response, we observed transient induction of P21 transcript following Cas9:sgRNA RNP electroporation to CD34+ HSPCs, with peak levels between 4 and 8 hours after electroporation (Extended Data Fig. 6c). Since we did not observe a difference in human chimerism in xenotransplant recipients, it appeared unlikely that this DNA damage response had a major impact on HSPC engraftment potential. In pluripotent stem cells, clones with P53 mutation or inhibition have been reported to have a selective advantage following gene editing[17]. We performed targeted deep sequencing of edited CD34+ HSPCs using a clinically approved 95-gene sequencing panel designed to identify recurrent somatically acquired hematologic malignancy-associated mutations, including *TP53* among loci tested[18]. We did not observe variant alleles at *TP53* or any other of the hematologic malignancy-associated loci in the edited HSPCs (Supplementary Table 6). Together, these data indicate an absence of detectable genotoxicity.

To determine whether this optimized *BCL11A* enhancer editing strategy could be effective in SCD, we obtained plerixafor-mobilized peripheral blood CD34+ HSPCs from two patients[19–21]. We
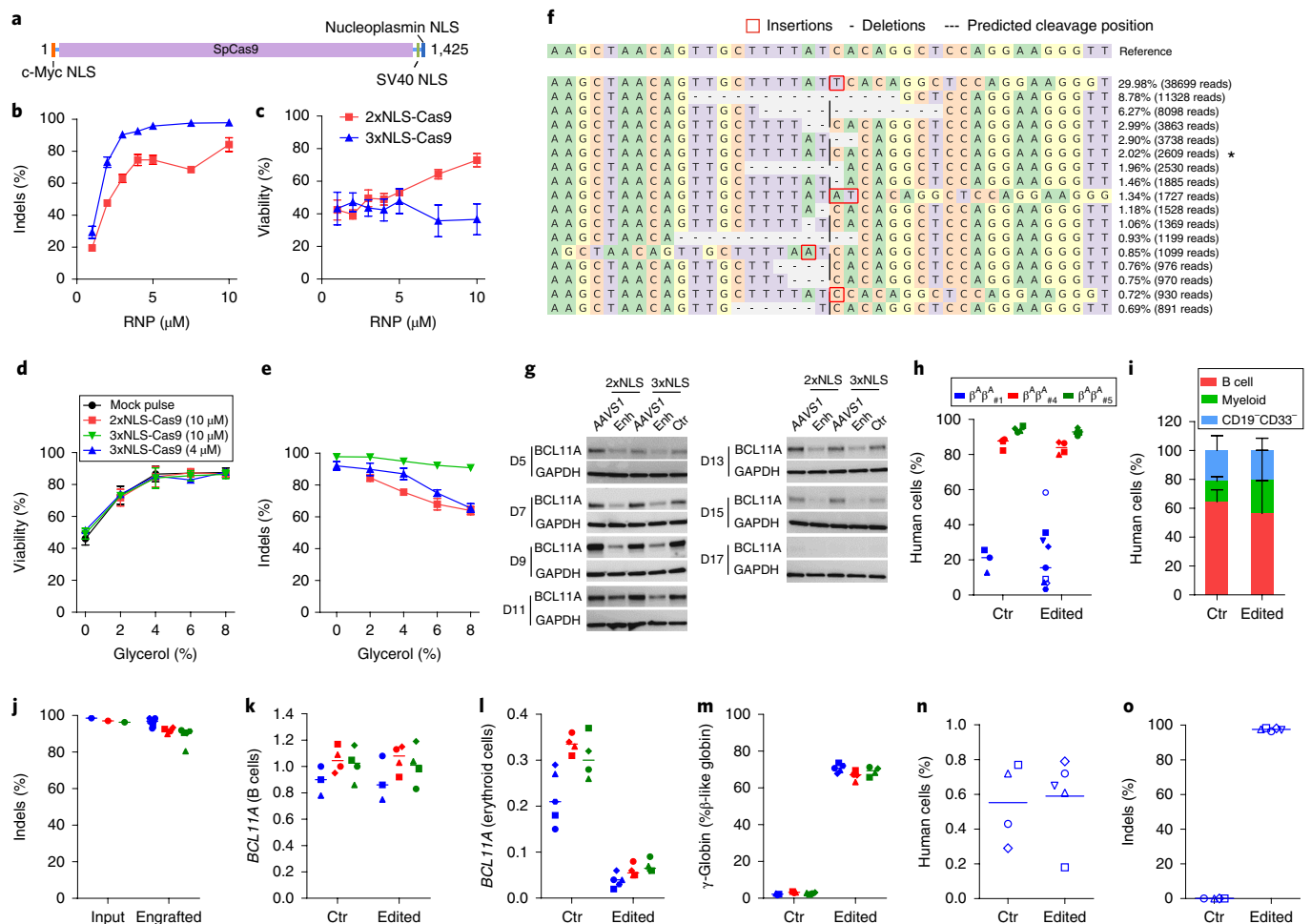
Fig. 2 | Highly efficient *BCL11A* enhancer editing in HSCs. a, Schematic of 3xNLS-SpCas9 protein (1,425 amino acids), with a c-Myc-like NLS at the N terminus and SV40 and nucleoplasmin NLSs at the C terminus. **b**, Dose-dependent editing of human *BCL11A* enhancer with 2xNLS-Cas9 or 3xNLS-Cas9 RNP. **c**, Viability of CD34+ HSPCs after electroporation with 2xNLS-Cas9 and 3xNLS-Cas9. **d**, Viability of CD34+ HSPCs after electroporation with RNP and glycerol. **e**, Indel frequencies of CD34+ HSPCs after electroporation with RNP and glycerol. Error bars indicate s.d. ($n = 3$ replicates with three independent healthy donors in **b–e**). **f**, Summary of the most frequent indels by deep sequencing following 3xNLS-Cas9 RNP *BCL11A* enhancer editing of CD34+ HSPCs. The asterisk indicates an unedited allele. **g**, Western blot analysis showing reduction of BCL11A protein after editing of human *BCL11A* enhancer with 2xNLS-Cas9 or 3xNLS-Cas9 RNP (MS-sgRNA-*AAVS1* or MS-sgRNA-1617) at indicated days of in vitro differentiation. Blots are cropped. BCL11A was observed at ~120 kDa, and GAPDH at ~37 kDa. **h–j**, NBSGW mice were transplanted with 3xNLS-Cas9 RNP (coupled with MS-sgRNA-1617) edited CD34+ HSPCs from three independent healthy donors (β^Aβ^A_{#1}, β^Aβ^A_{#4} and β^Aβ^A_{#5}). Bone marrow (BM) cells collected 16 weeks after transplantation were analyzed by flow cytometry for human cell chimerism (**h**), multilineage reconstitution from β^Aβ^A_{#1} (**i**) in BM, as well as the indel frequencies determined by TIDE analysis (**j**). **k–m**, RT–qPCR analysis of *BCL11A* expression in sorted human B cells (**k**) or human erythroid cells (**l**) and β-like globin expression in sorted human erythroid cells (**m**) from NBSGW mice transplanted with 3xNLS RNP edited CD34+ HSPCs. **n**, BM from one mouse each engrafted with unedited control or edited cells (β^Aβ^A_{#1}) was transplanted to secondary NBSGW mice, and BM was analyzed for human cell chimerism after 16 weeks. **o**, Indel frequencies within human *BCL11A* enhancer in BM 16 weeks after secondary transplantation. The median of each group with 3–9 mice in **h**, **j–o** is shown as a line. Data are plotted as mean ± s.d. for **b–e,i** and were analyzed using unpaired two-tailed Student's *t*-tests. Data are representative of three biologically independent replicates.

demonstrated 94.2–95.7% indels at the *BCL11A* enhancer following RNP electroporation of CD34+ HSPCs (Fig. 3a and Extended Data Fig. 7e). In vitro erythroid differentiated progeny showed 47.6% γ-globin in edited cells compared with 4.5% in unedited cells (Fig. 3b). Clonal analysis demonstrated that biallelic indels of the *BCL11A* enhancer, as short as 1 bp in length, resulted in robust induction of γ-globin, consistent with healthy donor results (total of 63 colonies analyzed from four donors; Fig. 3c, Supplementary Table 1, and Extended Data Figs. 1i and 3d,e). We observed similar human lymphoid, myeloid, and erythroid engraftment of edited and unedited SCD HSPCs (Fig. 3d and Extended Data Fig. 7b,c,g). There were similar results when edited cells were infused 1 or 2 d

following editing (Extended Data Fig. 7a–d). Edited cells showed 96.7% indels after 16 weeks of bone marrow engraftment compared with 95.0% indels in input HSPCs (Fig. 3e). *BCL11A* expression in erythroid cells was reduced by 83.1% while it was preserved in B lymphocytes (Fig. 3f,g). Edited bone marrow human erythroid cells expressed 59.0% γ-globin compared with 3.5% in unedited cells (Fig. 3h). The edited bone marrow SCD cells were able to support secondary transplantation to a similar level as unedited SCD cells, while maintaining a mean indel frequency of 98.1%, consistent with gene editing of self-renewing HSCs (Fig. 3i,j). CD34+ HSPCs were collected from the bone marrow of mice engrafted by SCD and healthy donor cells and subject to in vitro erythroid differentiation.
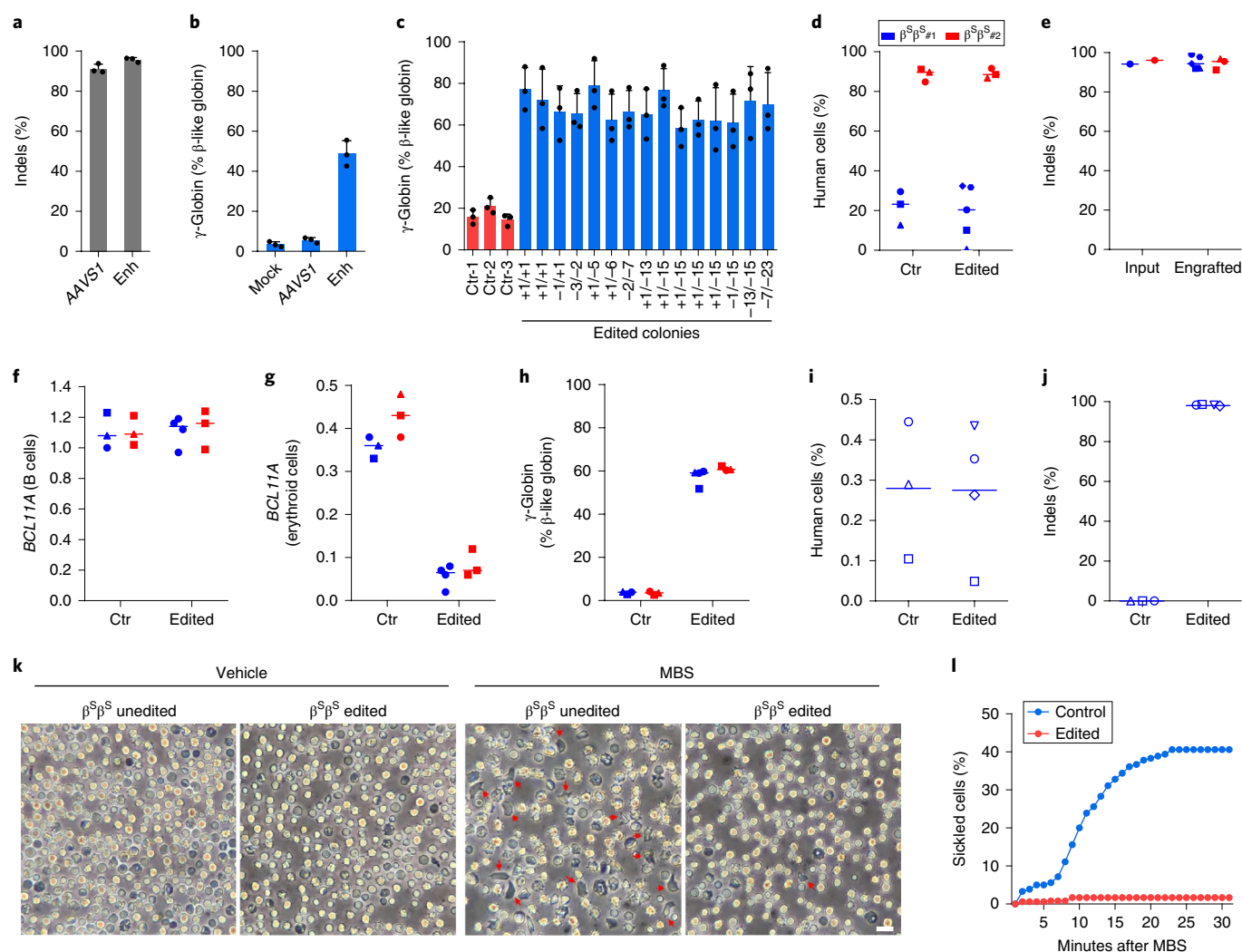
Fig. 3 | Editing *BCL11A* enhancer in SCD patient HSCs prevents sickling. a, Editing efficiency of 3xNLS-Cas9 coupled with MS-sgRNA-*AAVS1* for control and -1617 for *BCL11A* enhancer editing in $\beta^S\beta^S$ CD34+ HSPCs as measured by TIDE analysis. **b**, β-like globin expression in erythroid cells in vitro differentiated. Error bars indicate standard deviation ($n=3$ replicates). **c**, Genotyping and β-like globin expression analysis of erythroid cells derived from single colonies derived from unedited (ctr) or edited $\beta^S\beta^S$ CD34+ HSPCs. Error bars indicate s.d. ($n=3$ technical replicates per colony). **d,e**, NBSGW mice were transplanted with 3xNLS-Cas9 RNP (coupled with MS-sgRNA-1617) edited $\beta^S\beta^S$ CD34+ HSPCs from two independent donors ($\beta^S\beta^S_{\#1}$ and $\beta^S\beta^S_{\#2}$). BM was collected 16 weeks after transplantation and analyzed for human cell chimerism (**d**), and the indel frequencies were determined by TIDE analysis (**e**). **f–h**, RT–qPCR analysis of *BCL11A* expression in sorted human B cells (**f**) or human erythroid cells (**g**) and β-like globin expression in human erythroid cells sorted from BM (**h**). **i**, BM from one mouse each engrafted with unedited control or edited cells ($\beta^S\beta^S_{\#1}$) from control mouse shown with black circle and edited mouse with blue triangle symbols in **d,e**) were transplanted to four secondary NBSGW mice. After 16 weeks, BM was analyzed for human cell chimerism by flow cytometry. **j**, Indel frequencies within human *BCL11A* enhancer in BM 16 weeks after secondary transplantation. Median of each group with 3–4 mice in **d–j** is shown as line. **k**, Phase-contrast microscopy imaging of enucleated erythroid cells in vitro differentiated from BM of NBSGW mice transplanted with unedited or *BCL11A* enhancer edited $\beta^S\beta^S_{\#1}$ CD34+ HSPCs with and without MBS treatment. Cells with sickled cell morphology are indicated with red arrows. Scale bar, 10 μm. **l**, Analysis of in vitro sickling. Images were taken every 1 min after MBS treatment. Results are shown as the percentage sickled cells at each time point. Data are plotted as mean ± s.d. for **a–c** and were analyzed using unpaired two-tailed Student's *t*-tests. Data are representative of three biologically independent replicates.

In all cases of *BCL11A* enhancer editing, HbF levels were elevated (Extended Data Fig. 8d). In healthy donor cells, HbF levels rose from 4.1% in unedited, to 35.9% in 3xNLS-Cas9 RNP edited cells, and in SCD patient cells, HbF levels rose from 13.9% to 47.5%. While unedited SCD enucleated erythroid cells derived from engrafting HSCs demonstrated robust in vitro sickling following sodium metabisulfite (MBS) treatment, edited SCD cells were resistant to sickling (Fig. 3k,l, Extended Data Fig. 7h, and Supplementary Videos 1 and 2).

Erythroid cells differentiated in vitro from the bone marrow of mice engrafted with 3xNLS-Cas9 edited cells showed more potent

induction of HbF compared with 2xNLS-Cas9 edited cells, consistent with greater persistence of edited alleles in repopulating HSCs (Extended Data Fig. 8a,d). Comparing all of the transplant results, there was a strong correlation (Spearman $r=0.99$, $P<0.0001$) between indel frequencies in input HSPCs compared with human cells engrafting the bone marrow after 16 weeks (Fig. 4a). With reduced RNP concentration, we observed disproportionate loss of indels from an HSC-enriched immunophenotype population compared with bulk HSPCs (Extended Data Fig. 8e). We found that the indel spectrum in repopulating cells was different from that in
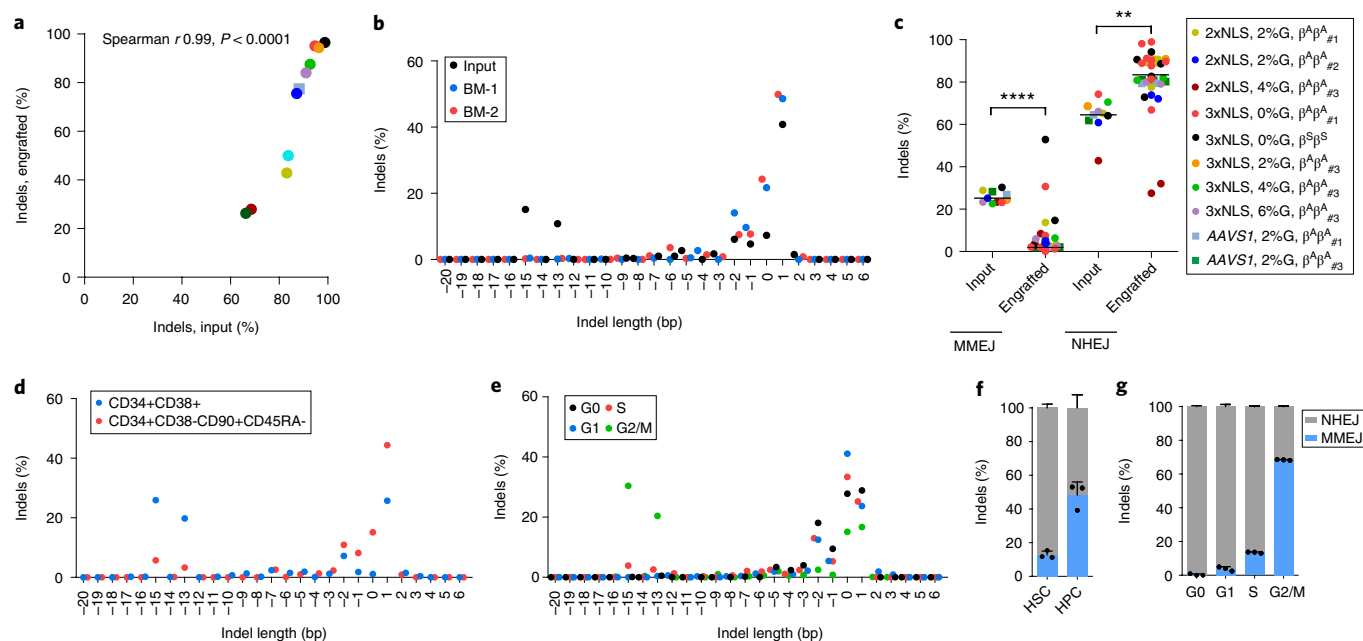
Fig. 4 | Persistence of NHEJ repaired alleles in HSCs. a, Correlation of indel frequencies of input HSPCs to indel frequencies of engrafted human cells in mice BM after 16 weeks. Each dot represents average indel frequencies of mice transplanted with the same input HSPCs. The legend denoting transplant is same as in **c**. The Spearman correlation coefficient (r) is shown. **b**, Indel spectrum of input cells from healthy donor β^{A}β$^A_{\#2}$ electroporated with 2xNLS-Cas9 (coupled with sgRNA-1617) supplemented with 2% glycerol and engrafted 16 week BM human cells. **c**, Relative loss of edited alleles repaired by MMEJ and gain of edited alleles repaired by NHEJ in mice BM 16 weeks after transplant. The indel spectrum was determined by deep sequencing analysis. Indel length from −8 to +6 bp was calculated as NHEJ, and from −9 to −20 bp as MMEJ. These data comprise 28 mice transplanted with 8 *BCL11A* enhancer edited inputs and 5 mice transplanted with 2 *AAVS1* edited inputs. The median of each group is shown as a line; **$P < 0.005$, ****$P < 0.0001$ as determined by Kolmogorov–Smirnov test. **d,e**, Indel spectra of HSPCs stained and sorted 2 h after RNP electroporation with 3xNLS-Cas9 with sgRNA-1617. HSPCs prestimulated for 24 h before electroporation. HSPCs were stained with CD34, CD38, CD90, CD45RA in **d** and with Pyronin Y, Hoechst 33342 in **e**. Indels were determined by Sanger sequencing with TIDE analysis after culturing cells for 4 d after sorting. Relative loss of edited alleles repaired by MMEJ and gain of edited alleles repaired by NHEJ at *BCL11A* enhancer and *AAVS1* in sorted enriched HSCs (**f**) or G0 phase cells (**g**) is shown. Data are plotted as mean ± s.d. for **f,g** and analyzed using unpaired two-tailed Student's *t*-tests. Data are representative of three biologically independent replicates.

input HSPCs (Fig. 4b and Extended Data Fig. 9a,b). For example, in HSPCs edited with 2xNLS-Cas9 with 2% glycerol the second and third most common indels were 15-bp and 13-bp deletions, comprising together 25.9% of alleles (Fig. 4b). These deletions were nearly absent in the engrafted cells, comprising together 1.0% of alleles. The 15-bp and 13-bp deletions were both predicted products of MMEJ repair[22] (Supplementary Table 7). These results suggested that NHEJ may be favored relative to MMEJ repair in the long-term repopulating HSC population relative to the bulk HSPC population. We classified each of the repair alleles, at *BCL11A* and *AAVS1*, as originating from NHEJ or MMEJ and compared their abundance in input HSPCs used for transplantation or in the engrafted cells resulting from these transplants. Together these data comprised ten independent transplants conducted with 33 recipient mice across *BCL11A* and *AAVS1*. We observed a significant decrease in the fraction of edited alleles repaired by MMEJ (median 25.2% versus 3.4%, $P < 0.0001$) and a concomitant increase in the fraction of edited alleles repaired by NHEJ (median 64.5% versus 81.0%, $P < 0.005$) in engrafted human cells compared with input HSPCs (Fig. 4c and Extended Data Fig. 9c). Since we observed similar results targeting *BCL11A* and *AAVS1*, it appeared unlikely there was locus-specific selection against MMEJ-edited repopulating cells. We speculated that quiescent HSCs would be relatively refractory to MMEJ repair, predominantly found in S and G2 phases of the cell cycle[23,24]. Comparing CD34$^+$ HSPCs immediately after thawing and following 24 hours in culture, we observed similar HSC immunophenotype by CD34, CD38, CD90, and CD45RA markers, increase of cell size, and shift from predominantly G0 to active cycling (Extended Data

Fig. 10). After 24 hours of prestimulation culture, we performed RNP electroporation and then 2 hours later sorted HSPCs into an enriched population of HSCs (CD34$^+$ CD38$^-$ CD90$^+$ CD45RA$^-$) compared with committed progenitors (CD34$^+$ CD38$^+$) or on the basis of G0, G1, S, and G2/M phase gates. Following an additional 4 d in culture, we determined the indel spectrum by sequence analysis. We observed depletion of the MMEJ alleles and enrichment of NHEJ alleles from the HSC compared with committed progenitor population for both *BCL11A* enhancer and *AAVS1* edited cells (Fig. 4d,f and Extended Data Fig. 9f). We found near-complete absence of MMEJ alleles from G0 and G1 phase HSPCs and enrichment in G2/M phase HSPCs after *BCL11A* enhancer or *AAVS1* editing (Fig. 4e,g and Extended Data Fig. 9g). These data suggest that quiescent and engrafting HSCs appear to favor NHEJ compared with MMEJ repair[23–25].

Previous experiments of genome editing in human HSPCs have shown variability in editing efficiency, specificity, and persistence in long-term engrafting HSCs (see Supplementary Table 8)[6,26–34]. Most prior studies have shown some reduction in indel frequency in engrafting cells compared with input HSPCs (Supplementary Table 8). The durability of therapeutic genome edits in the context of human hematopoietic autotransplant remains uncertain.

Here we address this concern by introducing therapeutic edits as a nearly complete reaction in long-term engrafting HSCs. We developed an optimized protocol for selection-free, HSC expansion-free *BCL11A* enhancer editing using modified synthetic sgRNA, SpCas9 protein with an additional NLS, and reformulated electroporation buffer in which we achieve ~95% therapeutic edits in healthy donor

and patient-derived engrafting cells without detectable genotoxicity. Even 1 bp indels following cleavage at core sequences within the *BCL11A* erythroid enhancer disrupt the GATA1-binding motif and are sufficient for robust HbF induction. Although we did not specifically investigate on-target large deletions following Cas9 cleavage[35], we have previously observed kilobase-scale deletions at the intronic *BCL11A* erythroid enhancer to result in erythroid-restricted loss of BCL11A expression[2–4].

Alternative plausible strategies for genome editing to ameliorate the β-hemoglobinopathies include targeting the β-globin cluster for gene repair or to mimic hereditary persistence of fetal hemoglobin alleles[26,27,30,36–39]. The efficiency of these homology- and microhomology-based maneuvers in HSCs in the absence of selection or HSC expansion remains to be determined, and in the case of gene repair the clinically relevant delivery of an extrachromosomal donor sequence presents an additional challenge. Ex vivo *BCL11A* enhancer editing approaching complete allelic disruption appears to be a realistic and scalable strategy with existing technology for durable HbF induction for the β-hemoglobinopathies. Emulating this efficiency could contribute to the success of industry-sponsored clinical trials of *BCL11A* enhancer editing using zinc finger nucleases (NCT03432364) and Cas9 (NCT03655678). Highly efficient HSC editing could be adapted for biological investigation and genetic amelioration of additional blood disorders[40].

Online content

Any methods, additional references, Nature Research reporting summaries, source data, statements of data availability and associated accession codes are available at https://doi.org/10.1038/s41591-019-0401-y.

References

1. Lettre, G. & Bauer, D. E. Fetal haemoglobin in sickle-cell disease: from genetic epidemiology to new therapeutic strategies. *Lancet* **387**, 2554–2564 (2016).
2. Bauer, D. E. et al. An erythroid enhancer of BCL11A subject to genetic variation determines fetal hemoglobin level. *Science* **342**, 253–257 (2013).
3. Canver, M. C. et al. BCL11A enhancer dissection by Cas9-mediated in situ saturating mutagenesis. *Nature* **527**, 192–197 (2015).
4. Smith, E. et al. Strict in vivo specificity of the Bcl11a erythroid enhancer. *Blood* **128**, 2338–2342 (2016).
5. Vierstra, J. et al. Functional footprinting of regulatory DNA. *Nat. Methods* **12**, 927–930 (2015).
6. Chang, K.-H. et al. Long-term engraftment and fetal globin induction upon BCL11A gene editing in bone-marrow-derived CD34+ hematopoietic stem and progenitor cells. *Mol. Ther. Methods Clin. Dev.* **4**, 137–148 (2017).
7. Kim, S., Kim, D., Cho, S. W., Kim, J. & Kim, J. Highly efficient RNA-guided genome editing in human cells via delivery of purified Cas9 ribonucleoproteins. *Genome Res.* **24**, 1012–1019 (2014).
8. Lin, S., Staahl, B., Alla, R. K. & Doudna, J. A. Enhanced homology-directed human genome engineering by controlled timing of CRISPR/Cas9 delivery. *Elife* **3**, 1–13 (2014).
9. Hendel, A. et al. Chemically modified guide RNAs enhance CRISPR-Cas genome editing in human primary cells. *Nat. Biotechnol.* **33**, 985–989 (2015).
10. Tsai, S.-F. et al. Cloning of cDNA for the major DNA-binding protein of the erythroid lineage through expression in mammalian cells. *Nature* **339**, 446–451 (1989).
11. McIntosh, B. E. et al. Nonirradiated NOD,B6.SCID Il2rγ⁻/⁻ Kit^{W41/W41} (NBSGW) mice support multilineage engraftment of human hematopoietic cells. *Stem Cell Rep.* **4**, 171–180 (2015).
12. Lu, X., Wood, D. K. & Higgins, J. M. Deoxygenation reduces sickle cell blood flow at arterial oxygen tension. *Biophys. J.* **110**, 2751–2758 (2016).
13. Estcourt, L., Fortin, P., Hopewell, S., Trivella, M. & Wang, W. C. Blood transfusion for preventing primary and secondary stroke in people with sickle cell disease. *Cochrane Database Syst. Rev.* **1**, CD003146 (2017).
14. Lin, S., Staahl, B., Alla, R. K. & Doudna, J. A. Enhanced homology-directed human genome engineering by controlled timing of CRISPR/Cas9 delivery. *Elife* **3**, 1–13 (2014).
15. Tsai, S. Q. et al. CIRCLE-seq: a highly sensitive in vitro screen for genome-wide CRISPR-Cas9 nuclease off-targets. *Nat. Methods* **14**, 607–614 (2017).
16. Haapaniemi, E., Botla, S., Persson, J., Schmierer, B. & Taipale, J. CRISPR–Cas9 genome editing induces a p53- mediated DNA damage response. *Nat. Med.* **24**, 927–930 (2018).
17. Ihry, R. J. et al. p53 inhibits CRISPR – Cas9 engineering in human pluripotent stem cells. *Nat. Med.* **24**, 939–946 (2018).
18. Kluk, M. J. et al. Validation and implementation of a custom next-generation sequencing clinical assay for hematologic malignancies. *J. Mol. Diagn.* **18**, 507–515 (2016).
19. Lagresle-Peyrou, C. et al. Plerixafor enables the safe, rapid, efficient mobilization of haematopoietic stem cells in sickle cell disease patients after exchange transfusion. *Haematologica* **103**, 778–786 (2018).
20. Boulad, F. et al. Safety and efficacy of plerixafor dose escalation for the mobilization of CD34+hematopoietic progenitor cells in patients with sickle cell disease: interim results. *Haematologica* **103**, 770–777 (2018).
21. Esrick, E. B. et al. Successful hematopoietic stem cell mobilization and apheresis collection using plerixafor alone in sickle cell patients. *Blood Adv.* **2**, 2505–2512 (2018).
22. Bae, S., Kweon, J., Kim, H. S. & Kim, J.-S. Microhomology-based choice of Cas9 nuclease target sites. *Nat. Methods* **11**, 705–706 (2014).
23. Truong, L. N. et al. Microhomology-mediated end joining and homologous recombination share the initial end resection step to repair DNA double-strand breaks in mammalian cells. *Proc. Natl Acad. Sci. USA* **110**, 7720–7725 (2013).
24. Sfeir, A. & Symington, L. S. Microhomology-mediated end joining: a back-up survival mechanism or dedicated pathway? *Trends Biochem. Sci.* **40**, 701–714 (2015).
25. Mohrin, M. et al. Hematopoietic stem cell quiescence promotes error-prone DNA repair and mutagenesis. *Cell Stem Cell* **7**, 174–185 (2010).
26. DeWitt, M. A. et al. Selection-free genome editing of the sickle mutation in human adult hematopoietic stem/progenitor cells. *Sci. Transl. Med.* **8**, 360ra134 (2016).
27. Dever, D. P. et al. CRISPR/Cas9 β-globin gene targeting in human haematopoietic stem cells. *Nature* **539**, 384–389 (2016).
28. Genovese, P. et al. Targeted genome editing in human repopulating haematopoietic stem cells. *Nature* **510**, 235–240 (2014).
29. Wang, J. et al. Homology-driven genome editing in hematopoietic stem and progenitor cells using ZFN mRNA and AAV6 donors. *Nat. Biotechnol.* **33**, 1256–1263 (2015).
30. Hoban, M. D. et al. Correction of the sickle-cell disease mutation in human hematopoietic stem/progenitor cells. *Blood* **125**, 2597–2604 (2015).
31. Ravin, S. S. De et al. CRISPR-Cas9 gene repair of hematopoietic stem cells from patients with X-linked chronic granulomatous disease. *Sci. Transl. Med.* **9**, 1–10 (2017).
32. Gundry, M. C. et al. Highly efficient genome editing of murine and human hematopoietic progenitor cells by CRISPR/Cas9. *Cell Rep.* **17**, 1453–1461 (2016).
33. Holt, N. et al. Human hematopoietic stem/progenitor cells modified by zinc-finger nucleases targeted to CCR5 control HIV-1 in vivo. *Nat. Biotechnol.* **28**, 839–847 (2010).
34. Diez, B. et al. Therapeutic gene editing in CD 34⁺ hematopoietic progenitors from Fanconi anemia patients. *EMBO Mol. Med.* **9**, 1574–1588 (2017).
35. Kosicki, M., Tomberg, K. & Bradley, A. Repair of CRISPR–Cas9-induced double-stranded breaks leads to large deletions and complex rearrangements. *Nat. Biotechnol.* **36**, 765–771 (2018).
36. Traxler, E. A. et al. A genome-editing strategy to treat β-hemoglobinopathies that recapitulates a mutation associated with a benign genetic condition. *Nat. Med.* **22**, 987–990 (2016).
37. Liu, N. et al. Direct promoter repression by BCL11A controls the fetal to adult hemoglobin switch. *Cell* **173**, 430–442.e17 (2018).
38. Martyn, G. E. et al. Natural regulatory mutations elevate fetal globin via disruption of BCL11A or ZBTB7A binding. *Nat. Genet.* **50**, 498–503 (2018).
39. Vakulskas, C. A. et al. A high-fidelity Cas9 mutant delivered as a ribonucleoprotein complex enables efficient gene editing in human hematopoietic stem and progenitor cells. *Nat. Med.* **24**, 1216–1224 (2018).
40. Xu, S. et al. Editing aberrant splice sites efficiently restores β-globin expression in β-thalassemia. *Blood* https://doi.org/10.1182/blood-2019-01-895094 (2019).

Author contributions

D.E.B. conceived and supervised this study. D.E.B. and Y.W. designed the experiments. Y.W. and J.Z. performed all experiments in human CD34^{+} HSPC, RNP editing, human CD34^{+} HSPC transplant, and engraftment analysis. D.E.B., Y.W., and J.Z. analyzed data. B.P.R., P.L., K.L., C.R., and S.A.W designed and purified 3xNLS-SpCas9 protein. D.M.D. assisted with hemoglobin HPLC analysis. E.B.E., J.P.M., D.A.W., and A.B. helped obtain plerixafor-mobilized SCD CD34^{+} HSPCs. C. Brugnara helped obtain β-thalassemia CD34^{+} HSPCs. C. Baricordi and L.B. assisted with flow cytometry of HSPCs. C. Brendel contributed to xenotransplant experiments and flow cytometry. C.R.L. and S.Q.T. performed CIRCLE-seq experiments and analyzed data. Q.Y., K.C., M.A.C., A.H.S., and L.P. performed computational data analyses. D.E.B. and Y.W. wrote the manuscript. All of the authors contributed to editing the manuscript.

Competing interests

Y.W., J.Z., S.A.W., and D.E.B. have applied for patents related to therapeutic gene editing, including US Patent applications nos. 13/72236, 15/572,523, 18/34618, and 18/43073.

Additional information

Extended data is available for this paper at https://doi.org/10.1038/s41591-019-0401-y.

Supplementary information is available for this paper at https://doi.org/10.1038/s41591-019-0401-y.

Reprints and permissions information is available at www.nature.com/reprints.

Correspondence and requests for materials should be addressed to D.E.B.

Publisher's note: Springer Nature remains neutral with regard to jurisdictional claims in published maps and institutional affiliations.

Methods

Cell culture. Human CD34^{+} HSPCs from mobilized peripheral blood of anonymized healthy donors were obtained from Fred Hutchinson Cancer Research Center, Seattle, Washington. Sickle cell disease patient and β-thalassemia patient CD34^{+} HSPCs were isolated from plerixafor-mobilized (for SCD, IRB P00023325, FDA IND 131740) or unmobilized (for β-thalassemia) peripheral blood following Boston Children's Hospital institutional review board (IRB) approval and informed patient consent. CD34^{+} HSPCs were enriched using the Miltenyi CD34 Microbead kit (Miltenyi Biotec). CD34^{+} HSPCs were thawed on day 0 into X-VIVO 15 (Lonza, 04–418Q) supplemented with 100 ng ml^{−1} human stem cell factor (SCF), 100 ng ml^{−1} human thrombopoietin (TPO), and 100 ng ml^{−1} recombinant human Flt3-ligand (Flt3-L). HSPCs were electroporated with Cas9 RNP 24 h after thawing and maintained in X-VIVO media with cytokines. For in vitro erythroid maturation experiments, 24 h after electroporation, HSPCs were transferred into erythroid differentiation medium (EDM) consisting of IMDM supplemented with 330 μg ml^{−1} holo-human transferrin, 10 μg ml^{−1} recombinant human insulin, 2 IU ml^{−1} heparin, 5% human solvent detergent pooled plasma AB, 3 IU ml^{−1} erythropoietin, 1% L-glutamine, and 1% penicillin/streptomycin. During days 0–7 of culture, EDM was further supplemented with 10^{-6} M hydrocortisone (Sigma), 100 ng ml^{−1} human SCF, and 5 ng ml^{−1} human IL-3 (R&D) as EDM-1. During days 7–11 of culture, EDM was supplemented with 100 ng ml^{−1} human SCF only as EDM-2. During days 11–18 of culture, EDM had no additional supplements, as EDM-3. Enucleation percentage and γ-globin induction were assessed on day 18 of erythroid culture.

In vitro transcription of sgRNAs. First, sgRNAs with T7 promoter were amplified by PCR from pX458 plasmid with specific primers (Supplementary Table 9) and in vitro transcribed using MEGAshortscript T7 kit (Life Technologies). After transcription, the sgRNAs were purified with MEGAclear kit (Life Technologies) according to manufacturer's instructions.

RNP electroporation. Electroporation was performed using Lonza 4D Nucleofector (V4XP-3032 for 20 μl Nucleocuvette Strips or V4XP-3024 for 100 μl Nucleocuvettes) as the manufacturer's instructions. 2xNLS-Cas9 was obtained from QB3 MacroLab, University of California, Berkeley. The modified synthetic sgRNA (2′-O-methyl-3′-phosphorothioate modifications in the first and last three nucleotides) was from Synthego. sgRNA concentration was calculated using the full-length product reporting method, which is threefold lower than the optical density reporting method. CD34^{+} HSPCs were thawed 24 h before electroporation. For 20 μl Nucleocuvette Strips, the RNP complex was prepared by mixing Cas9 (200 pmol) and sgRNA (200 pmol, full-length product reporting method) and incubating for 15 min at room temperature immediately before electroporation. For indicated experiments in which glycerol was supplemented, 30% glycerol solution was added to Cas9 protein before addition of sgRNA. HSPCs (5×10^4) resuspended in 20 μl P3 solution were mixed with RNP and transferred to a cuvette for electroporation with program EO-100. For 100 μl cuvette electroporation, the RNP complex was made by mixing 1,000 pmol Cas9 and 1,000 pmol sgRNA. HSPCs (5 M) were resuspended in 100 μl P3 solution for RNP electroporation as described above. The electroporated cells were resuspended with X-VIVO media with cytokines and changed into EDM 24 h later for in vitro differentiation. For mouse transplantation experiments, cells were maintained in X-VIVO 15 with SCF, TPO, and Flt3-L for 0–2 d as indicated before infusion.

Measurement of cell viability and indel frequencies. For the viability analysis, cell numbers were counted 48 h after electroporation, the viability was calculated as the cell number ratio of electroporated cells to mock control without electroporation. Indel frequencies were measured with cells cultured in EDM 5 d after electroporation. Briefly, genomic DNA was extracted using the Qiagen Blood and Tissue kit. *BCL11A* enhancer DHS +58 functional core was amplified with KOD Hot Start DNA polymerase and corresponding primers (Supplementary Table 9) using the following cycling conditions: 95 °C for 3 min; 35 cycles of 95 °C for 20 s, 60 °C for 10 s, and 70 °C for 10 s; 70 °C for 5 min. Resulting PCR products were subjected to Sanger sequencing. Sequencing traces were imported to TIDE software for indel frequency measurement with 40 bp decomposition window.

RT–qPCR quantification of γ-globin induction and *p21* expression. RNA isolation with RNeasy columns (Qiagen, 74106), reverse transcription with iScript cDNA synthesis kit (Bio-Rad, 170–8890), and RT–qPCR with iQ SYBR Green Supermix (Bio-Rad, 170–8880) was performed to determine γ-globin induction using primers amplifying *HBG1/2*, *HBB*, or *HBA1/2* cDNA (Supplementary Table 9). For quantification of *p21* mRNA, HSPCs were electroporated 24 h post-thawing, then were cultured in X-VIVO 15 medium plus cytokines as described above and collected at different time points post-editing.

Hemoglobin HPLC. Hemolysates were prepared from erythroid cells after 18 d of differentiation using Hemolysate reagent (5125, Helena Laboratories) and analyzed with D-10 Hemoglobin Analyzer (Bio-Rad) or HPLC in the clinical laboratory of the Brigham and Women's Hospital using clinically calibrated standards for the human hemoglobins.

Determination of BCL11A mRNA and protein level. Cells were directly lysed into the RLT plus buffer (Qiagen) for total RNA extraction according to manufacturer's instructions provided in the RNeasy Plus Mini Kit. *BCL11A* mRNA expression was determined by primers amplifying *BCL11A* or *CAT* as internal control (Supplementary Table 9). We used *CAT* as a reference transcript since it is both highly expressed and stable throughout erythroid maturation[41]. All gene expression data represent the mean of at least three technical replicates. For in vitro differentiation, *BCL11A* mRNA level was measured on day 11 unless otherwise indicated. BCL11A protein level was measured by western blot analysis as described previously[42] with the following antibodies: BCL11A (Abcam, ab19487), GAPDH (Cell Signaling, 5174s). The western blot results were quantified with ImageJ software.

Clonal culture of CD34^{+} HSPCs. Edited CD34^{+} HSPCs were sorted into 150 μl EDM-1 in 96-well round-bottom plates (Nunc) at one cell per well using FACSAria II. The cells were changed into EDM-2 media 7 d later in 96-well flat-bottom plates (Nunc). After an additional 4 d of culture, 1/10 of cells in each well were collected for genotyping analysis, the remaining cells were changed into 150–500 μl EDM-3 at 1 M ml^{−1} for further differentiation. After an additional 7 d of culture, 1/10 of the cells were stained with Hoechst 33342 for enucleation analysis, the remaining cells were collected with sufficient material for RNA isolation with RNeasy Micro Kit (74004, Qiagen) and RT–qPCR in technical triplicate or a single hemoglobin HPLC measurement per colony.

In vitro sickling and microscopy analysis. In vitro differentiated erythroid cells were stained with 2 μg ml^{−1} of the cell-permeable DNA dye Hoechst 33342 (Life Technologies) and the enucleated cells which are negative for Hoechst 33342 were FACS sorted and subjected to in vitro sickling assay. Sickling was induced by adding 500 μl freshly prepared 2% sodium MBS solution prepared in PBS into enucleated cells resuspended with 500 μl EDM-3 in a 24-well plate, followed by incubation at room temperature. Live cell images were acquired using a Nikon Eclipse Ti inverted microscope. Image acquisition was performed at room temperature and air in a 24-well plate. Time lapse images were recorded for 30 min with 10 s of intervals per sample.

Human CD34^{+} HSPC transplant and flow cytometry analysis. All animal experiments were approved by the Boston Children's Hospital Institutional Animal Care and Use Committee. CD34^{+} HSPCs were obtained from anonymized healthy donors or from β-hemoglobinopathy patients under protocols approved by the IRB of Boston Children's Hospital, with the informed consent of all participants, and complying with relevant ethical regulations. NOD.Cg-*Kit*[W-41J] *Tyr*[+] *Prkdc*[scid] *Il2rg*[tm1Wjl] (NBSGW) mice were obtained from Jackson Laboratory (Stock 026622). Non-irradiated NBSGW female mice (4–5 weeks of age) were infused by retro-orbital injection with 0.2–0.8 M CD34^{+} HSPCs (resuspended in 200 μl DPBS) derived from healthy donors or SCD patients. Equal numbers of pre-electroporation CD34^{+} HSPCs were used for experiments comparing in vitro culture for 0, 1, or 2 d following electroporation. Bone marrow was isolated for human xenograft analysis 16 weeks post-engraftment. Serial transplants were conducted using retro-orbital injection of bone marrow cells from the primary recipients. For flow cytometry analysis of bone marrow cells were first incubated with Human TruStain FcX (422302, BioLegend) and TruStain fcX (anti-mouse CD16/32, 101320, BioLegend) blocking antibodies for 10 min, followed by the incubation with V450 Mouse Anti-Human CD45 Clone HI30 (560367, BD Biosciences), PE-eFluor 610 mCD45 Monoclonal Antibody (30-F11) (61–0451–82, Thermo Fisher), FITC anti-human CD235a Antibody (349104, BioLegend), PE anti-human CD33 Antibody (366608, BioLegend), APC anti-human CD19 Antibody (302212, BioLegend), and Fixable Viability Dye eFluor 780 for live/dead staining (65-0865-14, Thermo Fisher). Percentage human engraftment was calculated as hCD45^{+} cells/(hCD45^{+} cells + mCD45^{+} cells) × 100. B cells (CD19^{+}) and myeloid (CD33^{+}) lineages were gated on the hCD45^{+} population. Human erythroid cells (CD235a^{+}) were gated on mCD45^{−}hCD45^{−} population. For the staining with immunophenotype markers of HSCs, CD34^{+} HSPCs were incubated with Pacific Blue anti-human CD34 Antibody (343512, Biolegend), PE/Cy5 anti-human CD38 (303508, Biolegend), APC anti-human CD90 (328114, Biolegend), APC-H7 Mouse Anti-Human CD45RA (560674, BD Bioscience), and Brilliant Violet 510 anti-human Lineage Cocktail (348807, Biolegend). Cell cycle phase in live CD34^{+} HSPCs was detected by cytometry as described previously[43]. Cells were resuspended in pre-warmed HSPC medium. First, we added Hoechst 33342 to a final concentration of 10 μg ml^{−1} and incubated at 37 °C for 15 min. Then we added Pyronin Y directly to cells at a final concentration of 3 μg ml^{−1} and incubated at 37 °C for 15 min. After washing with PBS, we performed flow cytometric analysis or cell sorting. Cell sorting was performed on a FACSAria II machine (BD Biosciences).

Amplicon deep sequencing. For indel frequencies or off-target analysis with deep sequencing, *BCL11A* enhancer loci or potential off-target loci were amplified with corresponding primers first (Supplementary Table 9). After another round of PCR with primers containing sample-specific barcodes and adapter, amplicons were sequenced for 2 × 150 paired-end reads with MiSeq Sequencing System

(Illumina). The deep sequencing data were analyzed by CRISPResso software[44]. In particular, we used a minimum alignment identity of 75%, window size of 2 bp around the cleavage site to quantify indels, an average PHRED quality score of 30, and excluded substitutions to limit potential false-positives. For OT10, in which the amplicon includes homologous genomic sequences, we used a minimum alignment identity of 90%.

Flow cytometry for F-cell, enucleation, and cell size analysis. Intracellular staining was performed as described previously. Cells were fixed with 0.05% glutaraldehyde (Sigma) for 10 min at room temperature and then permeabilized with 0.1% Triton X-100 (Life Technologies) for 5 min at room temperature. Cells were stained with anti-human antibodies for HbF (clone HbF-1 with FITC; Life Technologies) for 30 min in the dark. Cells were washed to remove unbound antibody before FACS analysis. Control cells without staining were used as negative control. For the enucleation analysis, cells were stained with 2 μg ml^{-1} of the cell-permeable DNA dye Hoechst 33342 (Life Technologies) for 10 min at 37 °C. The Hoechst 33342-negative cells were further gated for cell size analysis with Forward Scatter (FSC) A parameter. Median value of forward scatter intensity normalized by data from healthy donors collected at the same time was used to characterize the cell size.

Imaging flow cytometry analysis. In vitro differentiated D18 erythroid cells stained with Hoechst 33342 were resuspended with 150 μl DPBS for analysis with Imagestream X Mark II (Merck Millipore). Well-focused Hoechst-negative single cells were gated for circularity analysis with IDEAS software. Cells with circularity score above 15 were further gated to exclude cell debris and aggregates. No fewer than 2,000 gated cells were analyzed to obtain a median circularity score.

Preparation of 3xNLS-SpCas9. The plasmid expressing 3xNLS-SpCas9 was constructed in the pET21a expression plasmid (Novagen) and is available on Addgene (ID #114365). The recombinant *Streptococcus pyogenes* Cas9 with a 6xHis tag and c-Myc-like NLS at the N terminus[45], SV40, and nucleoplasmin NLS at the C terminus was expressed in *Escherichia coli* Rosetta (DE3)pLysS cells (EMD Millipore). Cells were grown at 37 °C to an OD$_{600}$ of ~0.2, then shifted to 18 °C and induced at an OD$_{600}$ of ~0.4 for 16 h with IPTG (1 mM final concentration). Following induction, cells were resuspended with Nickel-NTA buffer (20 mM Tris, 500 mM NaCl, 20 mM imidazole, 1 mM TCEP, pH 8.0) supplemented with HALT protease inhibitor and lysed with M-110s Microfluidizer (Microfluidics) following the manufacturer's instructions. The protein was purified with Ni-NTA resin and eluted with elution buffer (20 mM Tris, 250 mM NaCl, 250 mM imidazole, 10% glycerol, pH 8.0). Subsequently, 3xNLS-SpCas9 protein was further purified by cation exchange chromatography (column, 5 ml HiTrap-S; buffer A, 20 mM HEPES pH 7.5, 1 mM TCEP; buffer B, 20 mM HEPES pH 7.5, 1 M NaCl, 1 mM TCEP; flow rate, 5 ml min^{-1}; column volume, 5 ml) and size-exclusion chromatography on Hiload 16/600 Superdex 200 pg column (isocratic size-exclusion running buffer: 20 mM HEPES pH 7.5, 150 mM NaCl, 1 mM TCEP), then reconstituted in a formulation of 20 mM HEPES and 150 mM NaCl, pH 7.4.

CIRCLE-seq library preparation and data analysis. CIRCLE-seq experiments were performed as described previously[15]. In brief, purified genomic DNA was sheared to an average length of 300 bp, end repaired, A tailed, and ligated to uracil-containing stem-loop adapter. Adapter-ligated DNA was treated with Lambda Exonuclease (NEB) and *E. coli* Exonuclease I (NEB), followed by treatment with USER enzyme (NEB) and T4 polynucleotide kinase (NEB), then circularized with T4 DNA ligase, and treated with Plasmid-Safe ATP-dependent DNase (Epicentre) to degrade linear DNA. The circularized DNA was in vitro-cleaved by SpCas9 RNP coupled with sgRNA-1617. Cleaved products were A tailed, ligated with a hairpin adapter, treated with USER enzyme (NEB), and amplified by Kapa HiFi polymerase (Kapa Biosystems). The libraries were sequenced with 150 bp paired-end reads on an Illumina MiSeq instrument. The CIRCLE-seq sequencing data were analyzed by open-source Python package circleseq (https://github.com/tsailabSJ/circleseq).

Microhomology analysis. The sequence around the sgRNA-1617 target site of *BCL11A* enhancer region was uploaded to Microhomology-Predictor of CRISPR RGEN tools (http://www.rgenome.net/mich-calculator/) for microhomology sequence analysis. The 13-bp and 15-bp deletions have corresponding pattern scores of 283.2 and 261.0, respectively. The corresponding indel patterns were also identified by deep sequencing analysis. For *BCL11A* enhancer and *AAVS1*, indel sizes from −9 to −20 bp (representing most of the RGEN-predicted microhomology indels) were classified as MMEJ repaired alleles and indel sizes from −8 to +6 were classified as NHEJ repaired alleles.

Statistics and reproducibility. We utilized unpaired two-tailed Student's *t*-test, Pearson correlation, and Spearman correlation using GraphPad Prism, for analyses, as indicated in the figure legends.

Reporting Summary. Further information on research design is available in the Nature Research Reporting Summary linked to this article.

Data availability
The data that support the findings of this study are available within the paper and its supplementary information files. The deep sequencing data that support the findings of this study are publicly accessible from the National Center for Biotechnology Information Bioproject database with the accession number PRJNA517275, including the editing efficiency, pre- or post-mice-transplant data in Figs. 1–4 and the off-target assessment in Extended Data Fig. 6. The analytical results and statistics used to generate Figs. 1–4 and Extended Data Fig. 6 are provided in Supplementary Table 9. There are no restrictions on availability of the data from this study.

References
41. An, X. et al. Global transcriptome analyses of human and murine terminal erythroid differentiation. *Blood* **123**, 3466–3478 (2014).
42. Guda, S. et al. miRNA-embedded shRNAs for lineage-specific BCL11A knockdown and hemoglobin F induction. *Mol. Ther.* **23**, 1465–1474 (2015).
43. Eddaoudi, A., Canning, S. L. & Kato, I. in *Cellular Quiescence: Methods and Protocols* Vol. 1686 (ed. Lacorazza, H. D.) 49–57 (Humana Press, 2018).
44. Pinello, L. et al. CRISPResso: sequencing analysis toolbox for CRISPR-Cas9 genome editing. *Nat. Biotechnol.* **34**, 695–697 (2016).
45. Makkerh, J. P. S., Dingwall, C. & Laskey, R. A. Comparative mutagenesis of nuclear localization signals reveals the importance of neutral and acidic amino acids. *Curr. Biol.* **6**, 1025–1027 (1996).
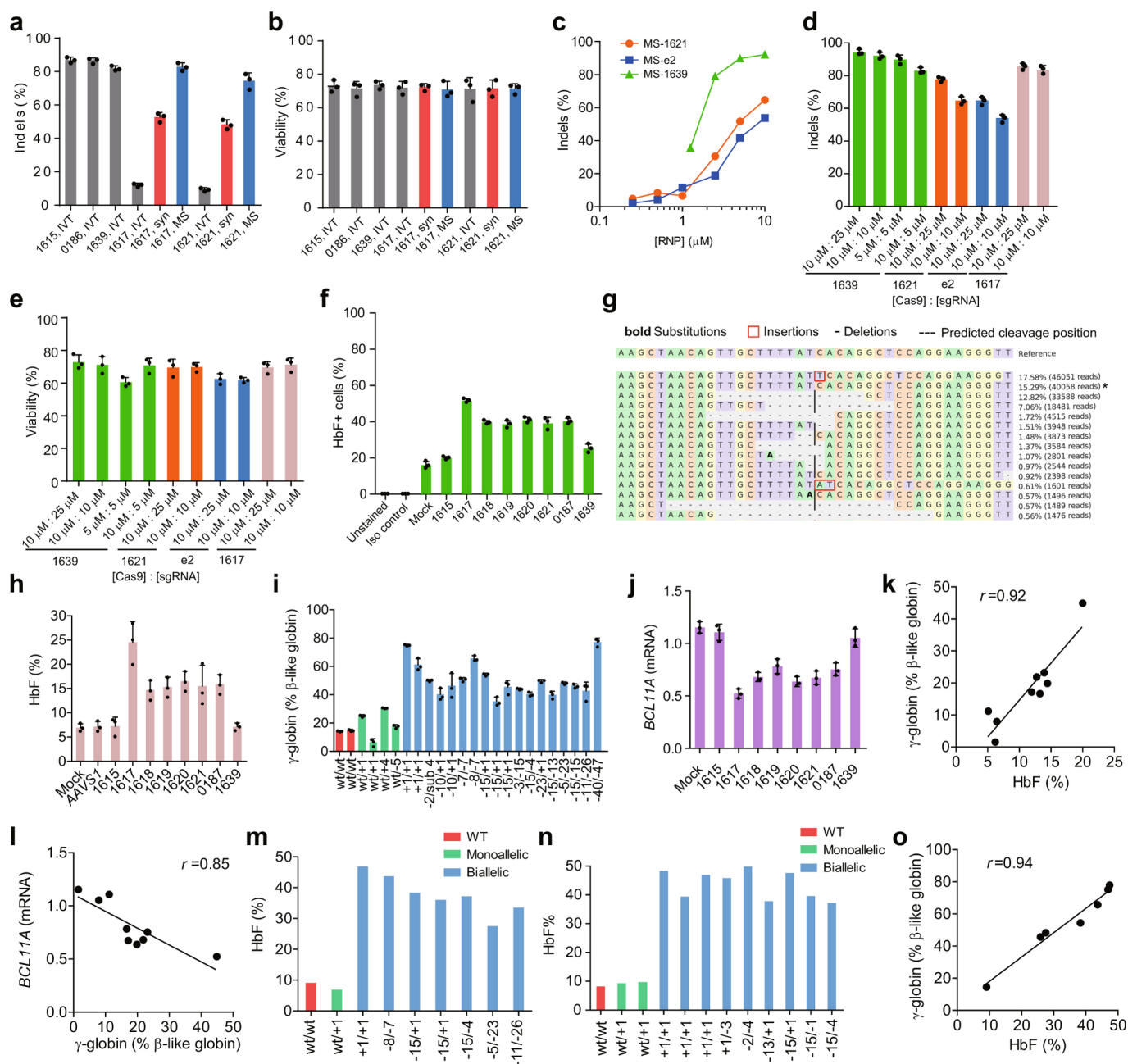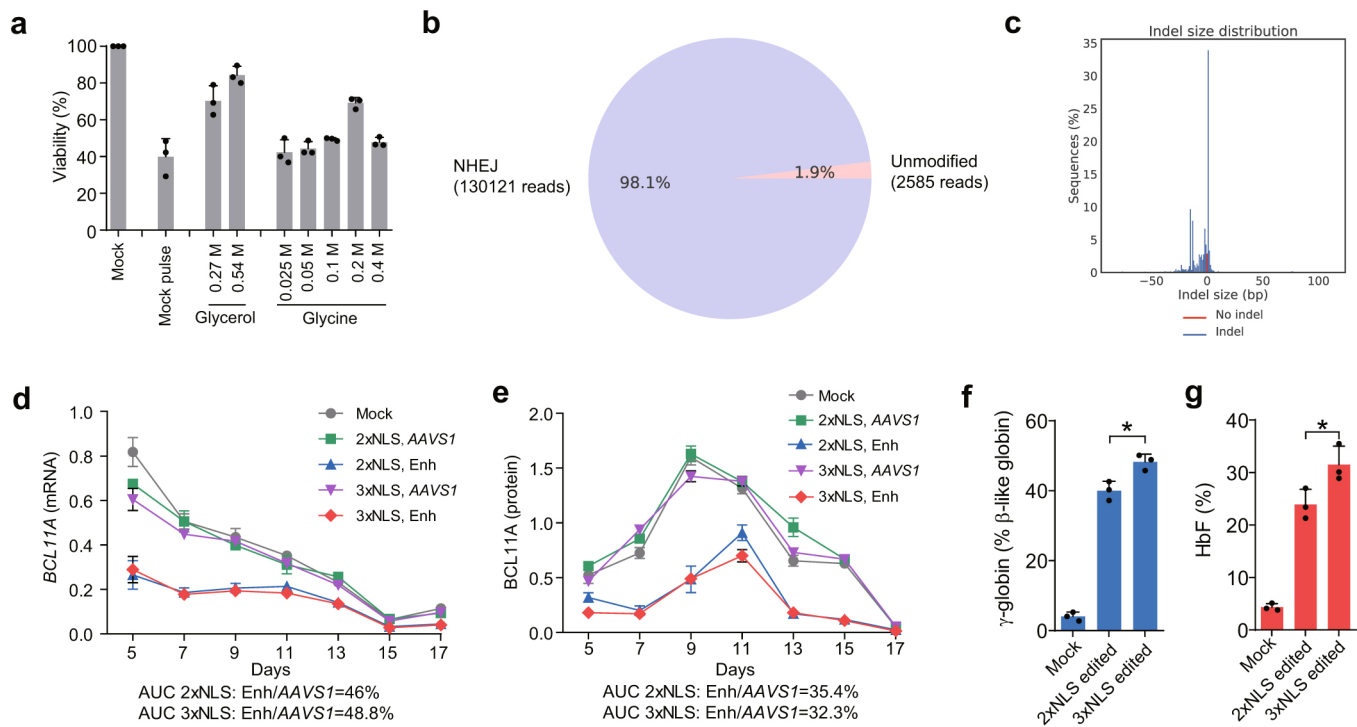
Extended Data Fig. 1 | Cas9 RNP dose-dependent editing of *BCL11A* enhancer for HbF induction in CD34⁺ HSPCs. a, Comparison of indel frequencies with in vitro transcribed (IVT), synthetic (syn) and modified synthetic (MS) sgRNAs in CD34⁺ HSPCs by TIDE analysis. **b**, Comparison of viability of CD34⁺ HSPCs edited with in vitro transcribed (IVT), synthetic (syn) and modified synthetic (MS) sgRNAs. **c**, Dose-dependent editing rates with Cas9 coupled with MS-sgRNA-1617 and -1639 targeting *BCL11A* enhancer and -e2 targeting *BCL11A* exon2 in CD34⁺ HSPCs by TIDE analysis. **d**, Comparison of indel frequencies with different molar ratios of Cas9 to MS-sgRNA in CD34⁺ HSPCs by TIDE analysis. **e**, Comparison of viability of CD34⁺ HSPCs edited with different molar ratios of Cas9 to MS-sgRNA. **f**, Percentage HbF⁺ cells by flow cytometry analysis in erythroid cells in vitro differentiated from CD34⁺ HSPCs edited by RNP coupled with various sgRNAs (each targeting *BCL11A* enhancer). Error bars indicate standard deviation (*n* = 3 replicates). **g**, Summary of deep sequencing data derived from the Cas9 RNP (coupled with MS-sgRNA-1617) edited CD34⁺ HSPCs. Asterisk indicates unedited allele. **h**, HbF induction by HPLC analysis in erythroid cells in vitro differentiated from RNP edited CD34⁺ HSPCs. **i**, Genotyping and β-like globin expression analysis of clonal erythroid cells derived from single CD34⁺ HSPCs. Error bars indicate standard deviation (*n* = 3 technical replicates per colony). **j**, *BCL11A* expression in CD34⁺ HSPCs edited with Cas9 coupled with various MS-sgRNAs targeting *BCL11A* enhancer. Expression normalized to *CAT*, measured by RT–qPCR on day 11 of in vitro differentiation. Error bars indicate standard deviation (*n* = 3 replicates). **k**, Correlation of γ-globin mRNA expression determined by RT–qPCR versus HbF by HPLC. Black dots represent samples edited with 2xNLS-Cas9 coupled with various MS-sgRNAs. **l**, Correlation of *BCL11A* mRNA versus γ-globin mRNA determined by RT–qPCR. Black dots represent samples edited with 2xNLS-Cas9 coupled with various sgRNAs. **m,n**, Genotyping and HbF level by HPLC of clonal erythroid cells derived from single CD34⁺ cells from two independent healthy donors (β^A β^A_#1 in **m** and β^A β^A_#3 in **n** edited with MS-sgRNA-1617. **o**, Correlation of percentage γ-globin mRNA determined by RT–qPCR versus HbF by HPLC. Black dots represent single colonies edited with 2xNLS-Cas9 coupled with MS-sgRNA-1617. The Pearson correlation coefficient (*r*) is shown. In all panels, data are plotted as mean ± s.d. Data are representative of three biologically independent replicates.
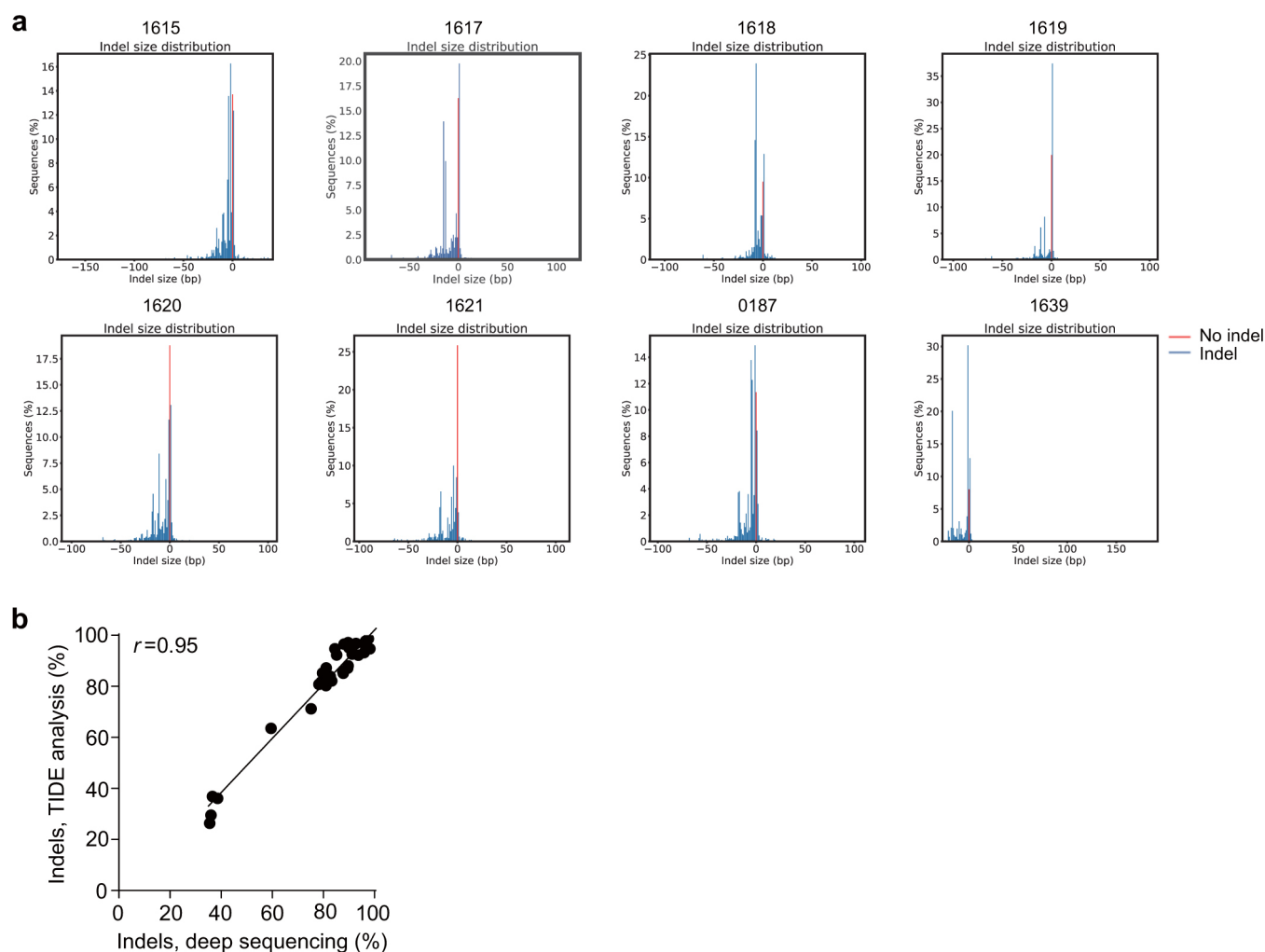
Extended Data Fig. 2 | Indel frequencies from deep sequencing. a. Frequency distribution of alleles with and without indels (shown in blue and red, respectively) from deep sequencing of CD34+ HSPCs edited with 2xNLS-Cas9 RNP with indicated MS-sgRNAs targeting *BCL11A* enhancer. **b**, Correlation of indel frequencies by deep sequencing versus indel frequencies by TIDE analysis. The Pearson correlation coefficient (*r*) is shown.
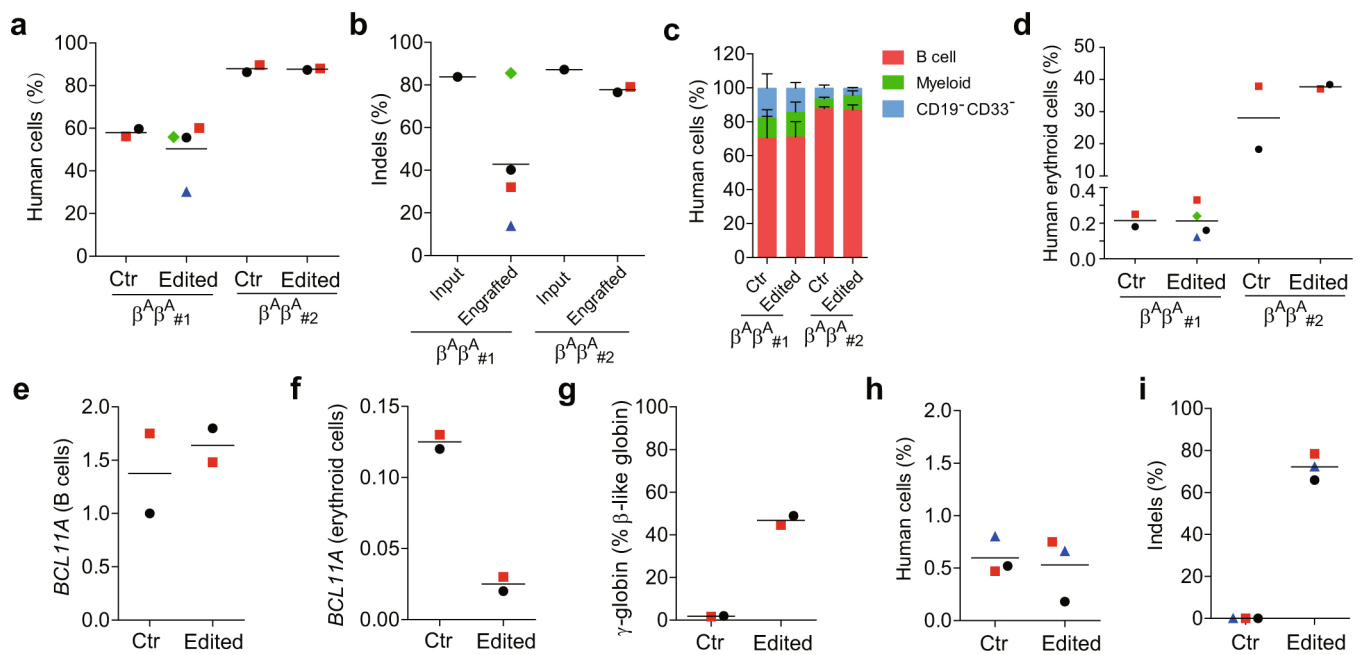
Extended Data Fig. 3 | Long-term multilineage engraftment of *BCL11A* enhancer edited HSPCs in immunodeficient mice. CD34+ HSPCs from two healthy donors were electroporated with 2xNLS-SpCas9 RNP (coupled with MS-sgRNA-1617) and transplanted into NBSGW mice. Non-electroporated cells were transplanted as controls. A total of 0.4 million cells per mouse were infused for donor $\beta^A\beta^A_{\#1}$, and 0.8 million cells per mouse for donor $\beta^A\beta^A_{\#2}$. **a**, Mouse bone marrow (BM) was analyzed for human cell chimerism by flow cytometry 16 weeks after transplantation, defined as %hCD45+/(%hCD45+ + %mCD45+) cells. Each symbol represents a mouse, and mean for each group is shown. **b**, Indels at the human *BCL11A* enhancer were determined by TIDE analysis in the input HSPCs before transplant and in the mouse bone marrow 16 weeks after transplant. Each engrafted dot represents one mouse, and mean for each group is shown. **c**, BM collected 16 weeks after transplantation was analyzed by flow cytometry for multilineage reconstitution (calculated as percentage of hCD45+ cells). **d**, BM collected 16 weeks after transplantation was analyzed by flow cytometry for CD235a+ erythroid cells (calculated as percentage of mCD45−hCD45− cells). **e–g**, Gene expression analysis by RT–qPCR in human cells (from donor $\beta^A\beta^A_{\#2}$) from BM of engrafted mice. *BCL11A* expression normalized by *CAT* in human B cells (**e**) or human erythroid cells (**f**) sorted from BM of engrafted mice, and β-like globin expression (**g**) by RT–qPCR in human erythroid cells sorted from BM. **h**, BM from one engrafted mouse with unedited control or edited cells (from donor $\beta^A\beta^A_{\#1}$) were transplanted to three secondary NBSGW mice each (control mouse shown with black circle and edited mouse with green diamond symbol in **a**,**b**,**d**. After 16 weeks, BM was analyzed for human cell chimerism by flow cytometry. **i**, Indel frequencies within human *BCL11A* enhancer in BM 16 weeks after secondary transplantation. Each symbol represents an individual recipient mouse. Data are plotted as mean ± s.d. for **c**. Median of each group with 2–4 mice is shown as line for the other panels.

Extended Data Fig. 4 | Highly efficient editing of *BCL11A* enhancer in CD34⁺ HSPCs. a, Dose-dependent viability enhancement with glycerol or glycine after electroporation. 0.27 M = 2% glycerol, 0.2 M = 1.5% glycine. **b**, Quantification of editing frequency from deep sequencing of CD34⁺ HSPCs edited with 3xNLS-Cas9 RNP with MS-sgRNA-1617. **c**, Length distribution of alleles with and without indels (shown in blue and red, respectively) from deep sequencing of the 2xNLS-Cas9 RNP with MS-sgRNA-1617. **d,e**, Reduction of *BCL11A* mRNA by RT–qPCR or protein by western blot after editing of human *BCL11A* enhancer with 2xNLS-Cas9 or 3xNLS-Cas9 RNP with MS-sgRNA-*AAVS1* or -1617 on various days of in vitro differentiation. Relative areas under curve (AUCs) are indicated. **f,g**, β-like globin expression by RT–qPCR and HbF level by HPLC in erythroid cells in vitro differentiated from 3xNLS-Cas9 RNP coupled with MS-sgRNA-1617 edited CD34⁺ HSPCs. All data represent the mean ± s.d. Statistically significant differences are indicated as follows: *$P < 0.05$ as determined by unpaired *t*-test. $P = 0.0152$ for **f**, 0.0443 for **g**. In all panels, data are plotted as mean ± s.d. and analyzed using unpaired two-tailed Student's *t*-tests. Data are representative of three biologically independent replicates.
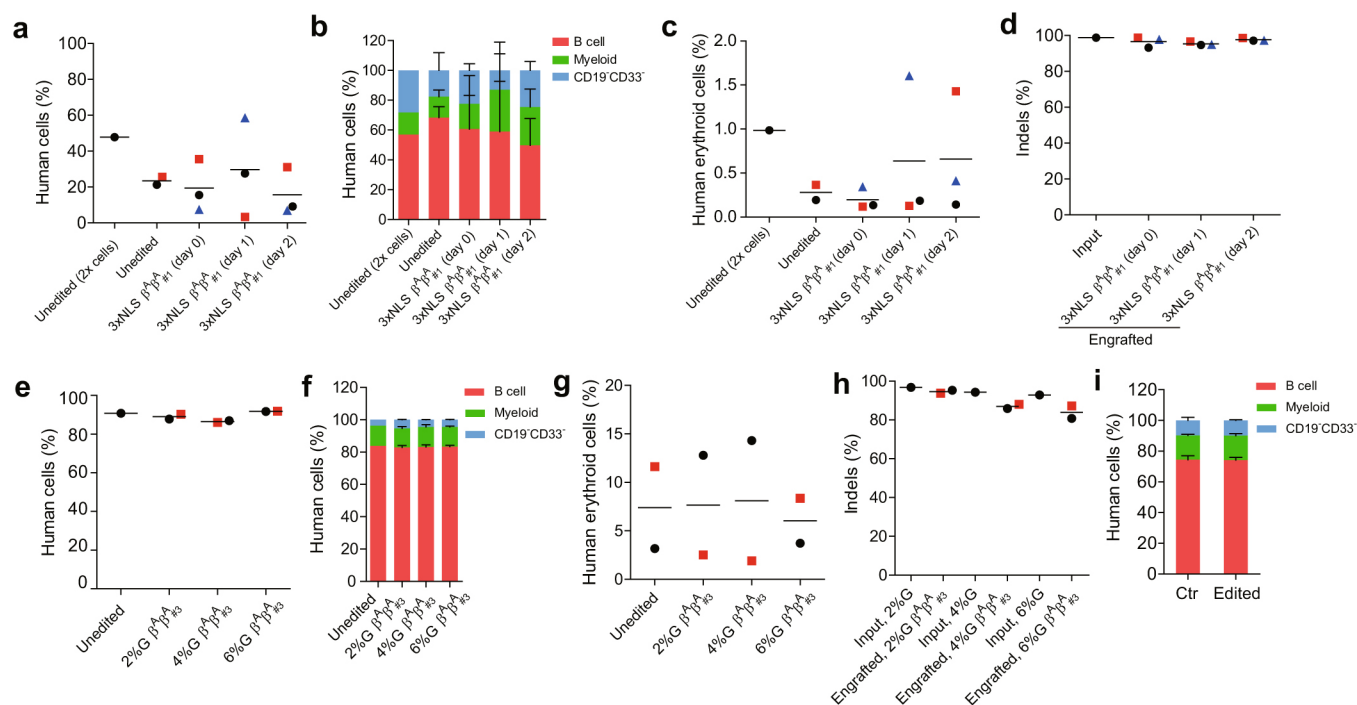
Extended Data Fig. 5 | Long-term multilineage reconstituting HSCs edited with 3xNLS-Cas9. a–d, NBSGW mice were transplanted with 3xNLS-Cas9 RNP with MS-sgRNA-1617 edited healthy donor CD34$^+$ HSPCs 2 h (day 0), 24 h (day 1) or 48 h (day 2) after electroporation. BM was collected 16 weeks after transplantation and analyzed by flow cytometry for human cell chimerism (**a**), multilineage reconstitution (**b**), or human erythroid cells (**c**) in BM, as well as indel frequencies determined by TIDE analysis (**d**). **e–h**, NBSGW mice were transplanted with 3xNLS-Cas9 RNP with MS-sgRNA-1617 edited healthy donor CD34$^+$ HSPCs supplemented with 2%, 4%, or 6% glycerol for electroporation. BM was collected 16 weeks after transplantation and analyzed by flow cytometry for human cell chimerism (**e**), multilineage reconstitution (**f**), or human erythroid cells (**g**) in BM, as well as the indel frequencies determined by TIDE analysis (**h**). **i**, Multilineage reconstitution analysis of BM collected from mice engrafted with control or edited CD34$^+$ HSPCs (from donor β^{A}β$^A_{\#4}$). Error bars indicate standard deviation. Data are plotted as mean ± s.d. for **b,f,i**. Median of each group with 1–3 mice is shown as line for the other panels.
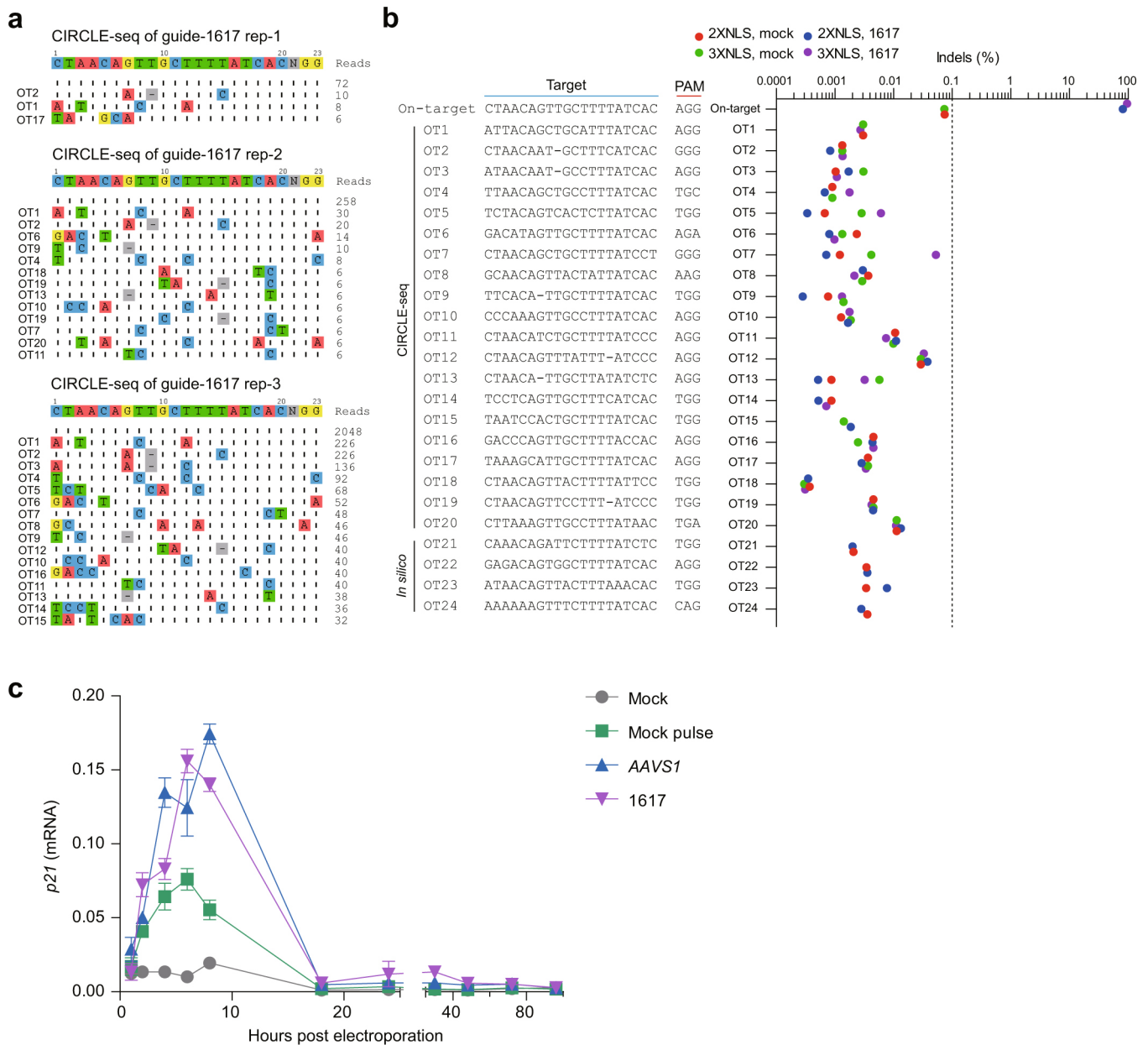
Extended Data Fig. 6 | Off-target analysis of human CD34+ HSPCs edited by SpCas9 RNP targeting *BCL11A* enhancer. a, Off-target sites detected by CIRCLE-seq for MS-sgRNA-1617 targeting human *BCL11A* enhancer. **b**, Deep sequencing analysis of potential off-target sites detected by CIRCLE-seq or in silico computational prediction within human CD34+ HSPCs edited by 2xNLS-Cas9 or 3xNLS-Cas9 RNP (coupled with MS-sgRNA-1617) targeting *BCL11A* enhancer. On-target sequence is at the *BCL11A* enhancer. Dotted line at 0.1% denotes sensitivity of deep sequencing to detect indels. **c**, RT–qPCR analysis of *p21* expression after gene editing. Relative expression to *GAPDH* is shown. Data are plotted as mean ± s.d. and representative of three biologically independent replicates.
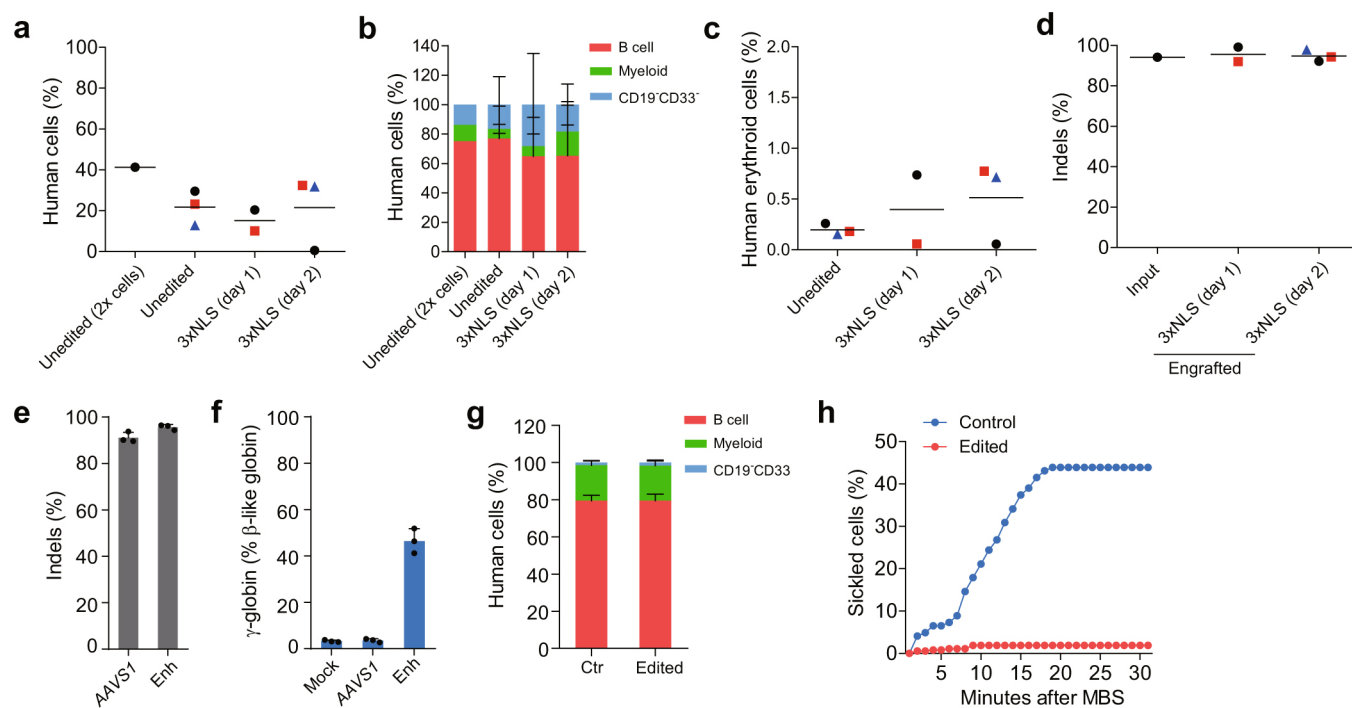
Extended Data Fig. 7 | Editing of *BCL11A* enhancer in SCD patient ($\beta^S\beta^S$) HSPCs. a–d, NBSGW mice were transplanted with 3xNLS-Cas9 RNP with MS-sgRNA-1617 edited $\beta^S\beta^S_{\#1}$ CD34$^+$ HSPCs 24 h (day 1) or 48 h (day 2) after electroporation. BM was collected 16 weeks after transplantation and analyzed by flow cytometry for human cell chimerism (**a**), multilineage reconstitution (**b**), or human erythroid cells (**c**) in BM, as well as the indel frequencies determined by TIDE analysis (**d**). Error bars indicate standard deviation. **e**, Editing efficiency of 3xNLS-Cas9 coupled with MS-sgRNA-*AAVS1* for control and -1617 for *BCL11A* enhancer editing in $\beta^S\beta^S_{\#2}$ CD34$^+$ HSPCs as measured by TIDE analysis. **f**, β-like globin expression by RT–qPCR analysis in erythroid cells in vitro differentiated from RNP edited $\beta^S\beta^S_{\#2}$ CD34$^+$ HSPCs. Error bars indicate standard deviation ($n=3$ replicates). **g**, Multilineage reconstitution analysis of BM collected from mice engrafted with control or edited CD34$^+$ HSPCs (from donor $\beta^S\beta^S_{\#2}$). **h**, Analysis of in vitro sickling of unedited control or edited enucleated $\beta^S\beta^S_{\#2}$ erythroid cells. Images were taken every 1 min after MBS treatment. Result shown as percentage sickled cells at each time point. Data are plotted as mean ± s.d. for **b**,**e**,**f**,**g**. Median of each group with 1–3 mice is shown as line for the other panels.
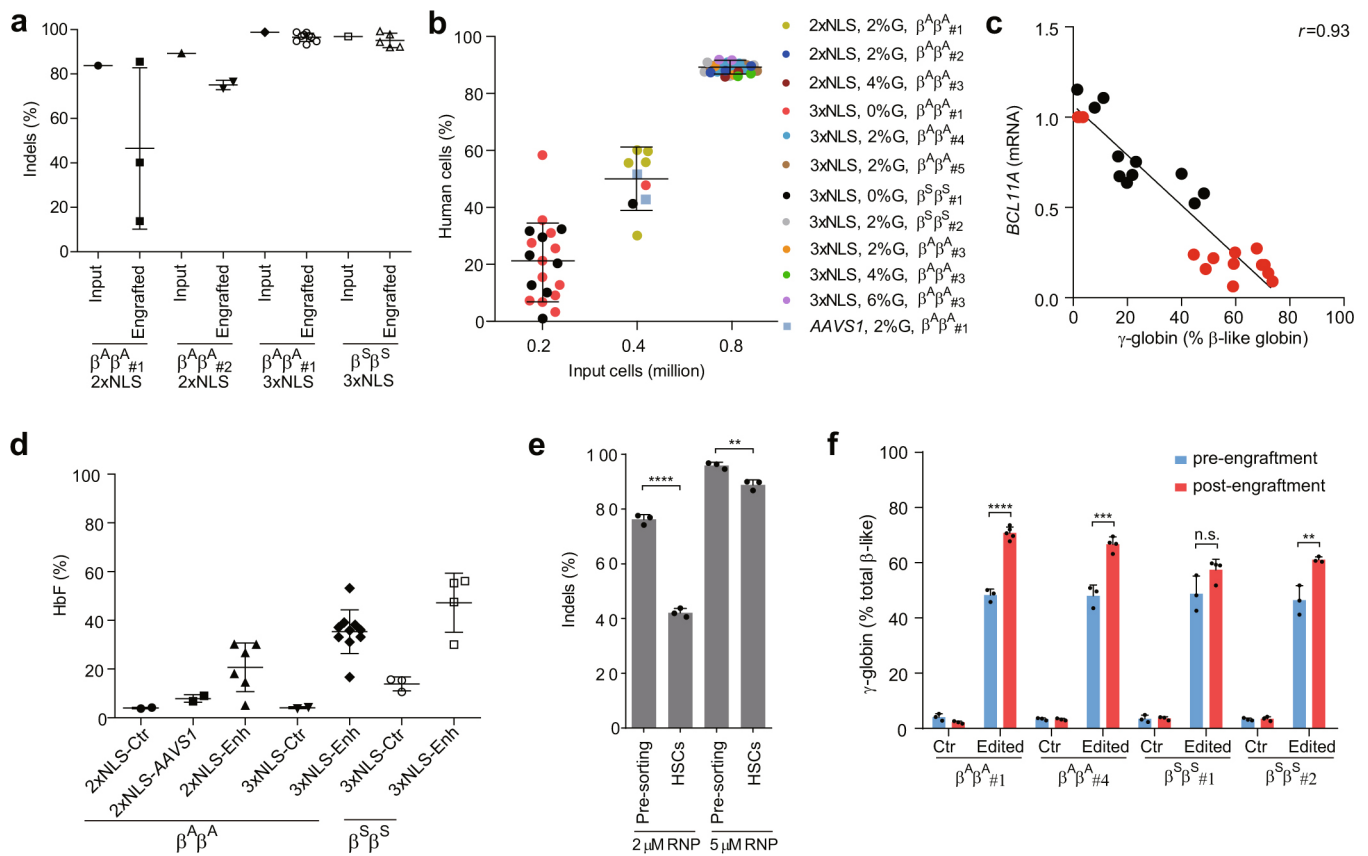
Extended Data Fig. 8 | Summary of engraftment analysis. a, Indel frequencies of indicated input HSPCs and engrafted human cells in 16 week BM. **b**. Correlation between input cell number and human engraftment rates in 16 week BM. **c**, Correlation of *BCL11A* mRNA versus γ-globin mRNA determined by RT–qPCR. Black dots represent erythroid cells from CD34+ HSPCs edited with SpCas9 coupled with various sgRNAs differentiated in vitro without engraftment; red dots represent erythroid cells sorted from mice BM engrafted from human CD34+ HSPCs edited with SpCas9 coupled with MS-sgRNA-1617. The Pearson correlation coefficient (*r*) is shown. **d**, BM cells (engrafted from donor βᴬβᴬ#1 and βˢβˢ#1) collected from engrafted mice were in vitro differentiated to human erythroid cells for HbF level analysis by HPLC. Each dot represents erythroid cells differentiated from BM of one mouse, and mean ± s.d. for each group is shown. **e**, Relative loss of indels in HSC-enriched CD34+ CD38− CD90+ CD45RA− sorted population compared with bulk pre-sorted HSPCs after editing by 2 μM or 5 μM RNP. All data represent the mean ± s.d. Statistically significant differences are indicated as follows: ****P < 0.0001, **P < 0.01 (P = 0.0046) as determined by unpaired *t*-test. **f**, Comparison of β-like globin expression by RT–qPCR between erythroid cells in vitro differentiated from RNP edited CD34+ HSPCs (pre-engraftment) and engrafted bone marrow (post-engraftment). Statistically significant differences are indicated as follows: ****P < 0.0001, ***P < 0.001 (P = 0.0006), **P < 0.01 (P = 0.0092) as determined by unpaired *t*-test. In all panels, data are plotted as mean ± s.d. and analyzed using unpaired two-tailed Student's *t*-tests. Data are from indicated number of mice for **a**,**b**,**d** or representative of three biologically independent replicates for **c**,**e**,**f**.
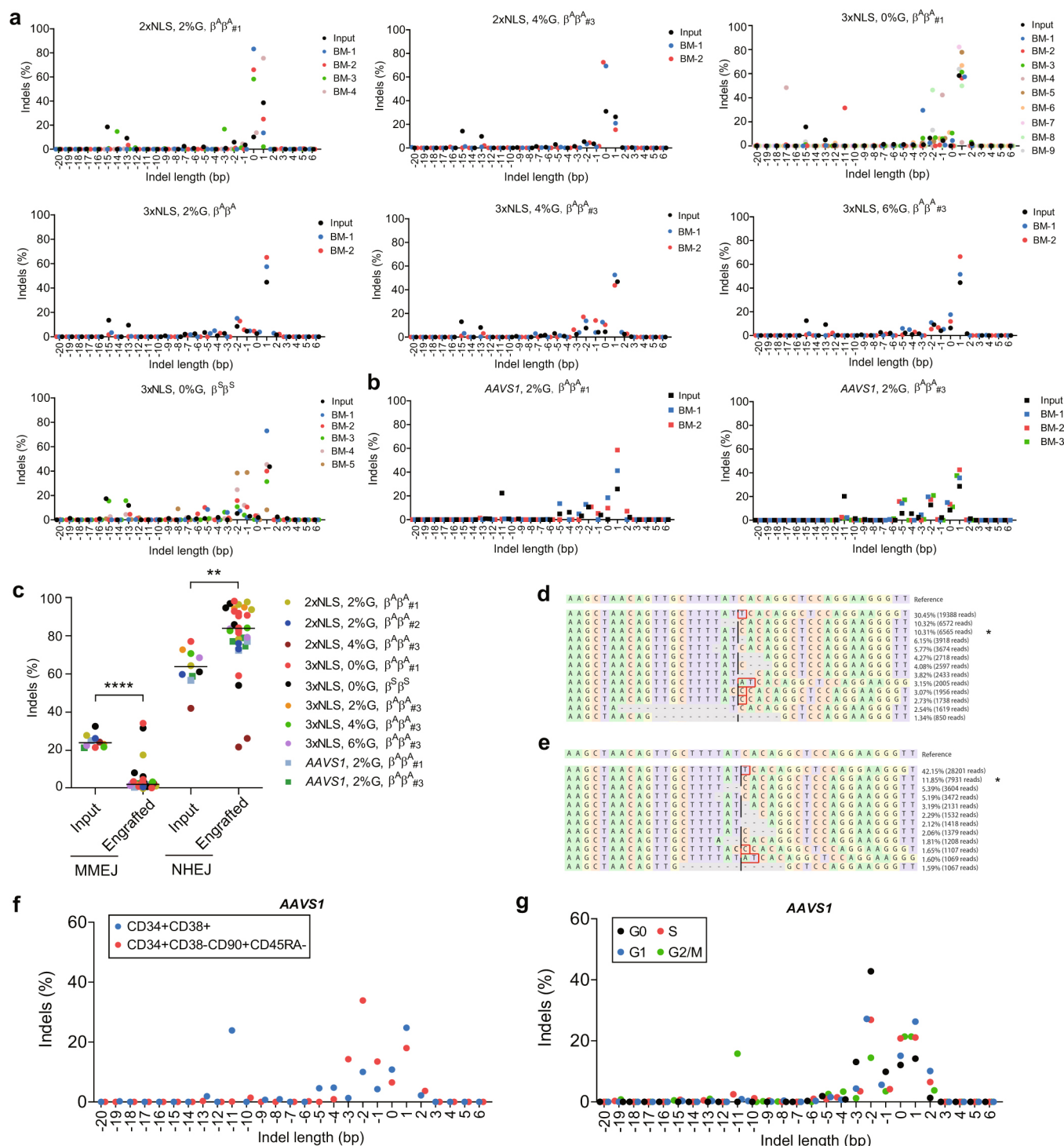
Extended Data Fig. 9 | Indel spectra of engrafted bone marrow and corresponding input cells. a,b, Indel spectra of engrafted bone marrow (BM) and corresponding input cells from four donors electroporated with 2xNLS-Cas9 or 3xNLS-Cas9 coupled with MS-sgRNA-1617 (**a**) or -*AAVS1* (**b**) supplemented with different concentration of glycerol (0%G to 6%G). **c,** Relative loss of edited alleles repaired by MMEJ and gain of edited alleles repaired by NHEJ in mice BM 16 weeks after transplant. The indel spectrum was determined by TIDE analysis. Indel length from −8 to +6 bp was calculated as NHEJ, and from −9 to −20 bp as MMEJ. These data comprise 28 mice transplanted with eight *BCL11A* enhancer edited inputs and five mice transplanted with two *AAVS1* edited inputs. Median of each group is shown as line, **P < 0.005, ****P < 0.0001 as determined by Kolmogorov–Smirnov test. **d,e,** Summary of most frequent indels by deep sequencing of bone marrow cells from primary recipient (**d**) and secondary recipient (**e**) engrafted with *BCL11A* enhancer edited CD34⁺ HSPCs. Asterisk indicates unedited allele. **f,g,** Indel spectra of HSPCs stained and sorted 2 h after RNP electroporation with 3xNLS-Cas9 with sgRNA-*AAVS1*. HSPCs prestimulated for 24 h before electroporation. HSPCs stained with CD34, CD38, CD90, CD45RA in **f** and with Pyronin Y, Hoechst 33342 in **g**. Indels determined by Sanger sequencing with TIDE analysis after culturing cells for 4 days after sort. Data are representative of three biologically independent replicates.
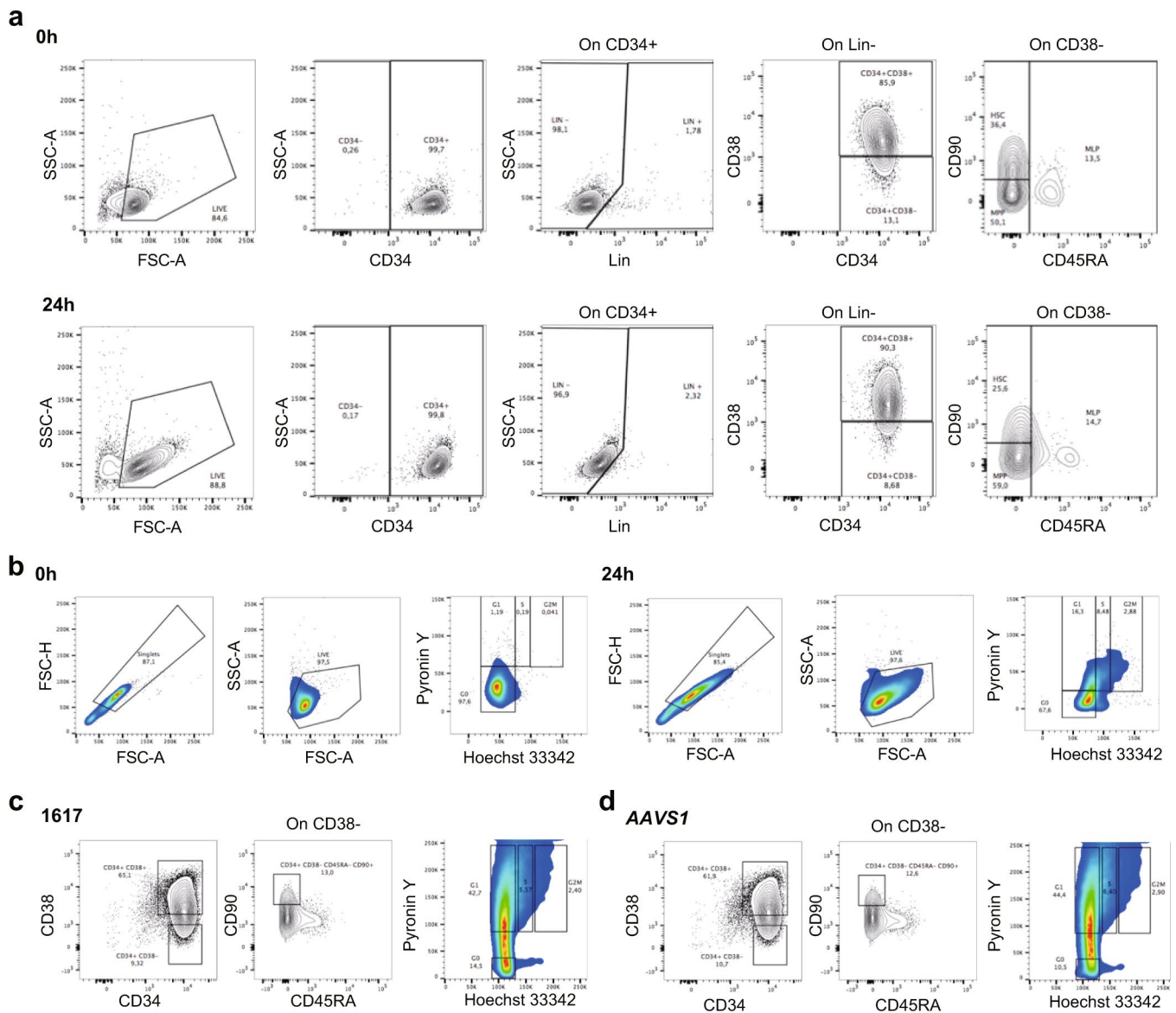
Extended Data Fig. 10 | Flow cytometry of CD34+ HSPCs with 24 h of culture. a–d, Cryopreserved G-CSF mobilized CD34+ HSPCs were stained with CD34, CD38, CD90, and CD45RA antibodies (in **a**), or stained with Hoechst 33342 and Pyronin Y (in **b**) at 0 h following thaw or after 24 h in culture with SCF, TPO and FLT3-L. HSPCs were electroporated with RNP with 3×-NLS-SpCas9 with *BCL11A* enhancer or *AAVS1* targeting sgRNA. After 2 h recovery, cells were stained with CD34, CD38, CD90, and CD45RA or with Hoechst 33342 and Pyronin Y, and sorted according to gates as shown in **c** and **d**.

Corresponding author(s): Daniel E. Bauer

Reporting Summary

Nature Research wishes to improve the reproducibility of the work that we publish. This form provides structure for consistency and transparency in reporting. For further information on Nature Research policies, see Authors & Referees and the Editorial Policy Checklist.

Statistical parameters

When statistical analyses are reported, confirm that the following items are present in the relevant location (e.g. figure legend, table legend, main text, or Methods section).

n/a	Confirmed	
☐	☒	The exact sample size (n) for each experimental group/condition, given as a discrete number and unit of measurement
☐	☒	An indication of whether measurements were taken from distinct samples or whether the same sample was measured repeatedly
☐	☒	The statistical test(s) used AND whether they are one- or two-sided *Only common tests should be described solely by name; describe more complex techniques in the Methods section.*
☐	☒	A description of all covariates tested
☐	☒	A description of any assumptions or corrections, such as tests of normality and adjustment for multiple comparisons
☐	☒	A full description of the statistics including central tendency (e.g. means) or other basic estimates (e.g. regression coefficient) AND variation (e.g. standard deviation) or associated estimates of uncertainty (e.g. confidence intervals)
☒	☐	For null hypothesis testing, the test statistic (e.g. F, t, r) with confidence intervals, effect sizes, degrees of freedom and P value noted *Give P values as exact values whenever suitable.*
☐	☒	For Bayesian analysis, information on the choice of priors and Markov chain Monte Carlo settings
☒	☐	For hierarchical and complex designs, identification of the appropriate level for tests and full reporting of outcomes
☐	☒	Estimates of effect sizes (e.g. Cohen's d, Pearson's r), indicating how they were calculated
☐	☒	Clearly defined error bars *State explicitly what error bars represent (e.g. SD, SE, CI)*

Our web collection on statistics for biologists may be useful.

Software and code

Policy information about availability of computer code

Data collection	Described in the manuscript.
Data analysis	Described in the manuscript.

For manuscripts utilizing custom algorithms or software that are central to the research but not yet described in published literature, software must be made available to editors/reviewers upon request. We strongly encourage code deposition in a community repository (e.g. GitHub). See the Nature Research guidelines for submitting code & software for further information.

Data

Policy information about availability of data

All manuscripts must include a data availability statement. This statement should provide the following information, where applicable:

- Accession codes, unique identifiers, or web links for publicly available datasets
- A list of figures that have associated raw data
- A description of any restrictions on data availability

All the data are available.

Field-specific reporting

Please select the best fit for your research. If you are not sure, read the appropriate sections before making your selection.

☒ Life sciences   ☐ Behavioural & social sciences   ☐ Ecological, evolutionary & environmental sciences

For a reference copy of the document with all sections, see nature.com/authors/policies/ReportingSummary-flat.pdf

Life sciences study design

All studies must disclose on these points even when the disclosure is negative.

Sample size	At least three mice used per donor for xenotransplant.
Data exclusions	No data were excluded from the analyses.
Replication	All the experiments are replicated more than three times.
Randomization	Not relevant. All recipient mice were female, 4-5 weeks of age.
Blinding	Not relevant for objective measures.

Reporting for specific materials, systems and methods

Materials & experimental systems

n/a	Involved in the study
☐	☒ Unique biological materials
☐	☒ Antibodies
☒	☐ Eukaryotic cell lines
☒	☐ Palaeontology
☐	☒ Animals and other organisms
☐	☒ Human research participants

Methods

n/a	Involved in the study
☒	☐ ChIP-seq
☐	☒ Flow cytometry
☒	☐ MRI-based neuroimaging

Unique biological materials

Policy information about availability of materials

Obtaining unique materials	All unique materials used are readily available from the authors or from standard commercial sources.

Antibodies

Antibodies used	All antibodies used in this study were described in the manuscript and available from standard commercial sources.
Validation	Each antibody for the species and application is validated.

Animals and other organisms

Policy information about studies involving animals; ARRIVE guidelines recommended for reporting animal research

Laboratory animals	NOD.Cg-KitW-41J Tyr + Prkdcscid Il2rgtm1Wjl (NBSGW) female mice (4-5 weeks of age) were obtained from Jackson Laboratory (Stock 026622).
Wild animals	The study did not involve wild animals.
Field-collected samples	The study did not involve samples collected from the field.

Human research participants

Policy information about studies involving human research participants

Population characteristics	Beta-thalassemia and sickle cell disease patients from Boston Children's Hospital were used as CD34+ HSPC donors.
Recruitment	Beta-thalassemia subjects recruited sequentially from the thalassemia clinic. Sickle cell disease subjects already recruited for a study of plerixafor mobilization (NCT02989701).

Flow Cytometry

Plots

Confirm that:

☒ The axis labels state the marker and fluorochrome used (e.g. CD4-FITC).

☒ The axis scales are clearly visible. Include numbers along axes only for bottom left plot of group (a 'group' is an analysis of identical markers).

☒ All plots are contour plots with outliers or pseudocolor plots.

☒ A numerical value for number of cells or percentage (with statistics) is provided.

Methodology

Sample preparation	The sample preparation and biological source of the cells were described in the manuscript.
Instrument	Cell sorting and flow cytometry analysis was performed on a FACSAria II machine (BD Biosciences).
Software	The flow cytometry data were analyzed by flowJo 10 software.
Cell population abundance	The purity of the samples was determined by rerunning with flow cytometry.
Gating strategy	The gating strategy was described in the manuscript and previous publications.

☒ Tick this box to confirm that a figure exemplifying the gating strategy is provided in the Supplementary Information.